

A SIMPLE METHOD FOR THE SYNTHESIS OF PERDEUTERATED AROMATIC HYDROCARBONS AND HETEROCYCLIC COMPOUNDS

Steven B. Hawthorne, David J. Miller, Ted R. Aulich, and Sylvia A. Farnum

University of North Dakota Energy Research Center
Box 8213, University Station
Grand Forks, North Dakota 58202

ABSTRACT

A general method has been developed for the preparation of deuterated aromatic compounds that are useful for coal reaction studies and as internal standards for GC/MS analysis. The method requires little specialized equipment or synthesis expertise. A reaction mixture containing DCl, D₂O, and chromium is used to exchange deuterium for aromatic hydrogens at temperatures of 200° to 300°C. A single set of reaction conditions can be used to prepare a wide range of deuterated aromatics with nearly complete exchange of aromatic hydrogen for deuterium and little or no chemical degradation of the reactant. When a 20:1 molar ratio of deuterium to aromatic hydrogen was used the isotopic purity of most species tested including phenanthrene (isotopic purity of 94%), pyrene (95%), phenol (96%), dibenzofuran (96%), carbazole (94%), and dibenzothiophene (93%), approached the H/D exchange equilibrium of 95% in two to fifteen hours. The method also works well with complex mixtures as demonstrated by the deuteration of aromatics in a coal-derived anthracene oil.

INTRODUCTION

The use of deuterated aromatic organic compounds as internal standards for the evaluation of sample preparation procedures and for the analysis of complex samples using gas chromatography coupled with mass spectrometry (GC/MS) can greatly increase the accuracy of analytical results while often reducing the time required for the analysis. Deuterated compounds and mixtures are also useful for studying the fate of organic compounds in complex systems such as coal conversion reactions. Unfortunately, the widespread use of deuterated compounds is limited by their high cost and the lack of availability of many compound classes.

The purpose of this paper is to describe a general method for the synthesis of deuterated species that is applicable to several classes of aromatic compounds, requires minimal time and synthesis expertise, yields a chemically and isotopically pure product, uses simple and inexpensive equipment and reagents, and can be used with complex mixtures. This method also yields products with multiple deuteriums which is desirable to avoid the overlap in the mass spectra that occurs from ¹³C isotope peaks and (M-H)⁺ ions when unlabeled and monodeuterio-labeled compounds occur in the same sample (1). The synthesis is similar to the method of Werstiuk and Kadai (2-6) for the H/D exchange of aromatic protons with D₂O/DCl except that chromium is added to increase the rate of H/D exchange. The ability of this method to provide chemically and isotopically pure perdeuterated products was evaluated

for several aromatic hydrocarbons and O-, S-, and N-containing aromatics. The method was also used to produce perdeuterated derivatives of the components of a coal-derived anthracene oil.

EXPERIMENTAL

All reactions were performed in 10 mm o.d. (8 mm i.d.) x approximately 8 cm long pyrex glass tubes. One end of the tube was sealed with a flame before adding the reagents. The reaction mixture was then frozen in liquid nitrogen, the tube was evacuated using a small laboratory vacuum pump, and the tube was sealed with a flame. This procedure filled approximately one-half of the tube volume with reagents. The sealed tubes were then placed into a 1.3 cm o.d. x 15 cm stainless steel pipe. Before capping the pipe with "Swagelok" fittings, approximately 2 mL of water was added so that the pressure inside and outside of the glass reaction tube would be approximately equal during heating. As a safety measure, the stainless steel pipe was placed inside a containment vessel made from a one-inch diameter thick-walled iron pipe with threaded end caps. A small hole was drilled through one of the end caps to avoid a pressure increase in the containment vessel. The entire apparatus was then heated to 200-300°C for an appropriate time period in the oven of a gas chromatograph. Caution: Since chloride ion degrades the strength of stainless steel, the stainless steel pipe should be replaced if a glass tube breaks during the reaction. The deuteration reagent consisted of 4% DCl (by wt.) in D₂O (both > 99% isotopically pure) with 10 mg/mL chromium metal. Since the dissolution of the chromium metal evolves hydrogen gas, the addition of chromium was performed in a ventilated hood. After the chromium had dissolved (approximately one hour), the reagent mixture was purged briefly with helium to removed dissolved hydrogen. The reagent could then be stored indefinitely in a desiccator.

Unless otherwise noted, the deuteration of the individual pure compounds was performed using a weighed amount of approximately 100 mg of test species and an appropriate volume of deuteration reagent to give a 20:1 molar ratio of reagent deuterium to exchangeable protons. Each of the pure compounds was reacted at 300°C for 2 hr and/or 15 hr. If significant chemical degradation occurred at this temperature, an additional synthesis was performed at 200°C for 2 hr. The deuteration of the anthracene oil was performed using 50 mg of sample with 1.0 mL of deuteration reagent.

GC/MS analysis of the deuterated products was performed with a Hewlett-Packard model 5985B using a 30 m x 0.32 mm i.d. (1µm film thickness) DB-5 fused silica capillary column (J&W Scientific, Rancho Cordova, C.A.). All analyses were performed in the electron impact mode with 70 eV ionizing voltage. Isotopic purity of the products was calculated from the resultant spectra. Gas chromatography with flame ionization detection (FID) was performed on a Hewlett-Packard model 5890 GC with the same type of chromatographic column as used for GC/MS. Chemical purity of the starting materials and the products was determined by GC/FID analysis using gravimetrically prepared solutions of standard and product species. Proton NMR analyses of the deuterated products were performed on a Varian model XL-200. The deuterated products were dissolved in CD₂Cl₂ containing 0.25% tetramethylsilane.

Since most of the test compounds (except the N-containing bases) were not soluble in the reagent, quantitative recovery of the products was easily attained by pipetting off the liquid products or by removing the reagent from the solid products with a Pasteur pipette. The solid products were washed with water and dried to remove the residual reagent. The N-containing aromatic bases (aniline and quinoline) were removed from the reagent by making the reaction mixture basic with 2N NaOH and extracting with methylene chloride. Since the purpose of this synthesis method was to provide labeled products with deuterium substitution in chemically stable positions, the hydroxyl deuterium on the two phenols, and the two amine deuteriums on aniline were exchanged for protons from H₂O before being analyzed for their isotopic purity.

RESULTS AND DISCUSSION

The success of H/D exchange using the DCI/D₂O/chromium reagent in synthesizing perdeuterated aromatic compounds from several compound classes is shown in Table I. Mass spectra of several representative compounds before and after deuteration are shown in Figure 1. H/D exchanges with ethyl benzene, phenanthrene, pyrene, perylene, biphenyl, phenol, dibenzofuran, aniline, carbazole, and dibenzothiophene all approached equilibrium with the deuterium pool (assumed to be 95% isotopic purity based on the 20:1 molar ratio of D/H) in either two or 15 hours with no significant chemical degradation. The isotopic purity of those species that attain exchange equilibrium (95% isotopic purity) can be improved, if desired, by increasing the ratio of reagent D to exchangeable H or by performing multiple exchange reactions. Quinoline also showed no chemical degradation, but was only 73% isotopically pure after 15 hours. However, such products can still be useful for isotope dilution analysis. For example, the mass spectra of 73% isotopically pure quinoline-d₇ has a base peak of 134 compared to 129 for undeuterated quinoline and, since no detectable overlap in their mass spectra occurs in the molecular ion region, the 73% isotopically pure product is still useful as an internal standard (Figure 1). Longer reaction times and/or higher reagent D to reactant H ratios could be used to increase the isotopic purity.

Only three species, 2,4-dimethylphenol, anisole, and 2-methylthiophene, showed enough degradation that the synthesis at 300°C was judged to be unsuitable. Milder conditions of 200°C for 2 hr. were used for each of these species in an attempt to reduce degradation. Both 2,4-dimethylphenol and 2-methylthiophene were reasonably stable under these conditions and yielded products with isotopic purities of 89% and 85%, respectively (Table I). The methyl hydrogens of 2-methylthiophene exchanged readily and were included in the calculation of isotopic purity. Anisole continued to be converted to phenol even at these milder conditions with only 43% of the original anisole remaining after the reaction. Under these conditions, only three positions on anisole underwent significant H/D exchange. These positions were shown by 200 MHz proton NMR to be the ortho- and para-positions, as would be expected since the methoxy group activates those positions for electrophilic substitution. The same result is obtained when phenol undergoes the synthesis at 200°C for 2 hr. These results indicate that this method may be useful to produce aromatic compounds labeled at specific (ortho-, para- vs. meta-) positions by careful selection of the reaction temperature.

The use of this synthesis to produce perdeuterated derivatives in complex mixtures was demonstrated with a coal derived anthracene oil containing predominantly aromatic hydrocarbons. Figure 2 shows the results obtained when the anthracene oil underwent H/D exchange for 2 hours at 300°C. No detectable chemical degradation of the sample occurred as determined by a comparison of the GC/FID chromatograms of the oil before and after the synthesis. The molecular ion regions of the mass spectra obtained before and after the synthesis are shown for several representative species (Figure 2). The isotopic purities were naphthalene (97%), dibenzofuran (98%), dibenzothiophene (99%), phenanthrene (96%), and pyrene (97%). Aromatic compounds having aliphatic protons also showed nearly quantitative exchange of aromatic protons for deuterium, and some exchange of the aliphatic protons. For example, the base peak for 2-methylnaphthalene-d₇ (if only aromatic protons exchanged for D) would be at m/z 149. The intense peaks at m/z 151 and 152 show that some aliphatic protons also exchanged (Figure 2).

The results of the perdeuteration studies of pure compounds (Table I) and the anthracene oil demonstrate that the method presented here is useful for synthesizing perdeuterated aromatic compounds from several compound classes as well as in complex mixtures. All of the species that have been tested yield products with both high isotopic purity and (except for anisole) high chemical purity. The cost of the reagent is low (less than 20 dollars for this entire study) and the synthesis is simple to perform.

CREDIT

The authors would like to thank the U.S. Department of Energy for partial support of this work under contract number DE-FG22-86PC90911.

REFERENCES

1. Blom, K.; Schuhardt, J.; Munson, B. Anal. Chem. 1985, 57, 1986-1988.
2. Werstiuk, N.H.; Kadai, T. Can. J. Chem. 1973, 51, 1485-1486.
3. Werstiuk, N.H.; Kadai, T. Can. J. Chem. 1974, 52, 2169-2171.
4. Werstiuk, N.H.; Kadai, T. In "Proceedings of the First International Conference on Stable Isotopes in Chemistry, Biology, and Medicine"; Klein, P.K.; Peterson, S.V.; Eds; 1973, NTIS CONF-730525, pp. 13-19.
5. Werstiuk, N.H.; Timmins, G. Can. J. Chem. 1981, 59, 3218-3219.
6. Werstiuk, N.H.; Timmins, G. Can. J. Chem. 1981, 51, 1485-1486.

Table I
Synthesis of Perdeuterated Aromatic Compounds

	n ^a	Isotopic Purity (%)			Chemical Purity (%)		
		300°C 2 hr	300°C 15 hr	200°C 2 hrs	300°C 2 hr	300°C 15 hr	200°C 2 hr
ethylbenzene	5	50	97		100	100	
phenanthrene	10	94	94		100	95	
biphenyl	10	84	96		100	100	
pyrene	10	-	95		-	100	
perylene	12	-	95		-	100	
phenol	6	94	96	100 ^c	100	99	100
2,4-dimethylphenol	4			89	88	39	97 ^d
anisole	5	-	-	97 ^c	<5 ^d	<5 ^d	43 ^d
dibenzofuran	8	52	96		100	100	
aniline	7	95	96		100	77 ^d	
quinoline	7	29	73		100	100	
carbazole	8	93	94		94	89	
2-methylthiophene	6 ^b	-	-	85 ^b	e	e	89
dibenzothiophene	8	95	93		99	99	

^aThe number of exchangeable protons, n, is used for calculating the quantity of reagent required to give a D/H ratio of 20:1 in the reaction mixture.

^bAll six of the protons on 2-methylthiophene exchanged readily so n=6 was used to determine the quantity of deuteration reagent and for the calculation of isotopic purity.

^cIsotopic purity was based on 3 rather than 5 H/D exchanges (see text).

^dThe degradation product was phenol.

^eNo 2-methylthiophene or identifiable degradation product was recovered.

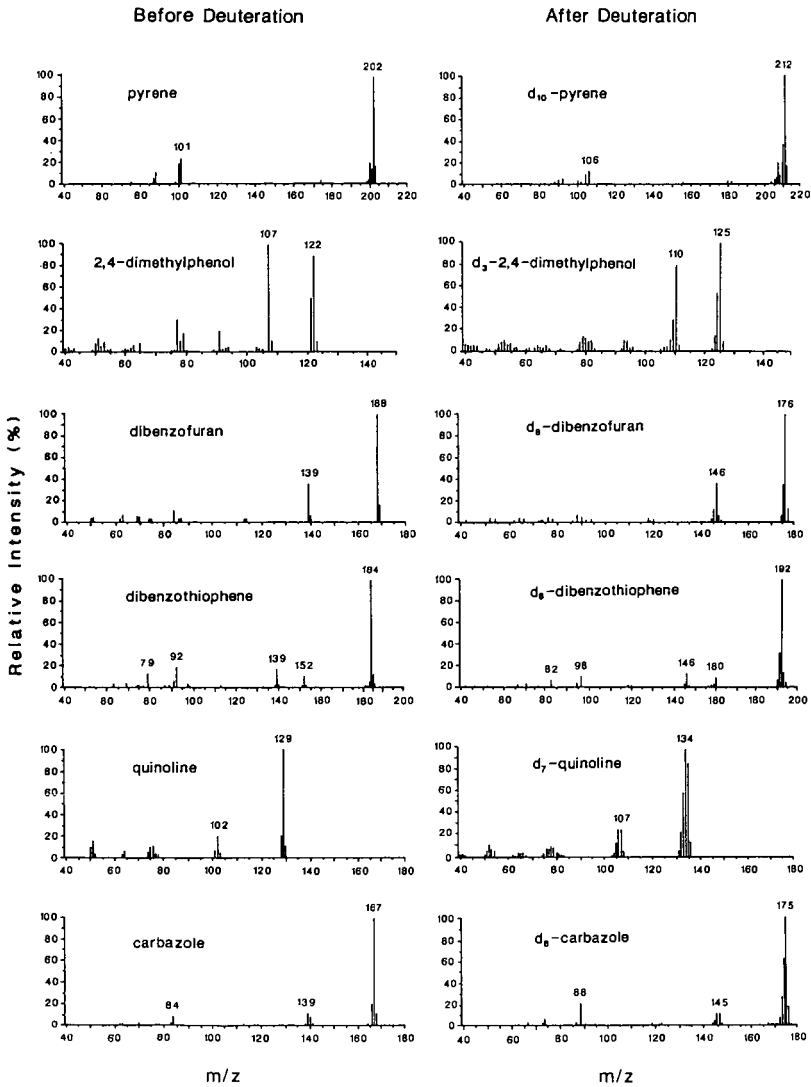


Figure 1: Electron impact mass spectra of representative PAH and O-, S-, and N- containing aromatics before (left side of figure) and after (right side) deuteration for 15 hours at 300°C. Isotopic and chemical purities are given in Table I.

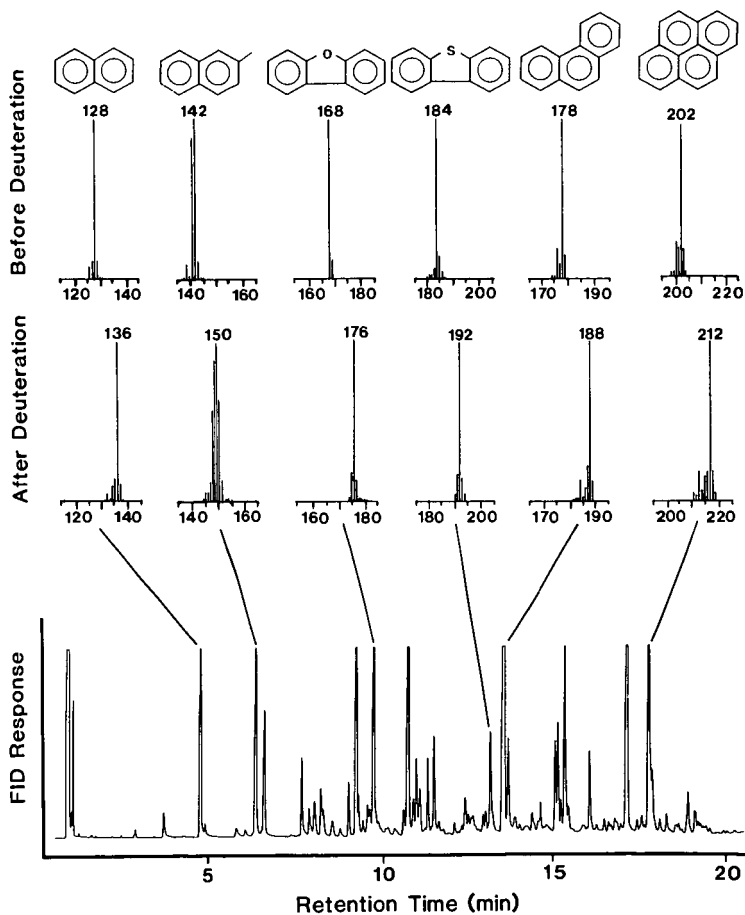


Figure 2: A comparison of the mass spectral molecular ion regions of representative species before (upper spectra) and after (lower spectra) deuteration of a coal-derived anthracene oil. Reaction conditions, isotopic purities, and gas chromatographic conditions are given in the text.

A New Method for Estimation of Activation Energies Associated with Coal Gasification Reactions

K. Raghunathan and R.Y.K. Yang
Department of Chemical Engineering
West Virginia University
Morgantown, WV 26506-6101

Kinetic studies of coal gasification and pyrolysis are important in the design and operation of gasification plants. In many of these studies, weight loss of a coal sample is continuously recorded, with a TGA for example, to produce conversion versus time data for a specific set of experimental conditions. Theoretical and empirical models are frequently used to represent those primary kinetic data. With a proper representation of the conversion data, other secondary kinetic data such as half-life and reactivity are evaluated. Characterization of coal, development of proper reaction rate models and estimation of its activation energy follow.

Mahajan et al. (1978) found that when the char conversion is plotted as a function of a dimensionless time τ , defined by $\tau = t/t_{1/2}$, where $t_{1/2}$ is the half-life of the reaction, gasification data for widely different experimental conditions can be represented by a single x versus τ curve. This unification approach has been used and confirmed by a number of researchers, e.g., Kasaoka et al. (1985) and Peng et al. (1986).

In this work we use the unification approach as the basis to develop a theoretical relation between half-life and average reactivity which is then verified experimentally. The relation in turn leads to the development of a simple and practical alternative for estimating the apparent activation energies of coal gasification and other types of reactions.

THEORY

Char conversion x depends on experimental variables such as temperature, pressure, etc., and it increases with gasification time. This may be represented symbolically as

$$x = f_0(T, P, \dots, t) \quad (1)$$

For each gasification run, with variables other than t being fixed, researchers usually fit the conversion-versus-time data rate expressions of the form

$$R_c = dx/dt = F(x) \quad (2)$$

where R_c is the char reactivity and x the char conversion.

According to the unification approach, when the data sets are normalized by replacing t by τ , a single x versus τ curve represents all the data, irrespective of the other experimental variables, reacting media and coal types. In other words, Eq. (1) becomes

$$x = f(\tau), \quad (3)$$

where f is the functional form of the unification curve. In this article, we show that this curve can be reduced even further, into a universal value, through the following discussion:

Eq. (3) may alternatively be presented as

$$\tau = g(x). \quad (4)$$

The above two equations are mathematical statements of the unification concept. From both equations,

$$dx/d\tau = f'(\tau) = f'\{g(x)\} = G(x) \quad (5)$$

Thus, $dx/d\tau$, the normalized reactivity is a function of conversion alone, and by averaging this reactivity over the entire conversion range, we remove the dependence of the normalized curve on conversion as well. Hence, if we define average normalized reactivity R_u as

$$R_u = \overline{dx/d\tau} = \frac{\int_0^1 (dx/d\tau) dx}{\int_0^1 dx} = \int_0^1 (dx/d\tau) dx = \int_0^1 G(x) dx \quad (6)$$

then, R_u is a universal constant.

Similar to Eq. (6), the average reactivity for a particular gasification run \bar{R}_C is

$$\bar{R}_C = \overline{dx/dt} = \int_0^1 (dx/dt) dx = \int_0^1 F(x) dx \quad (7)$$

which, as shown above, is a constant quantity unique to each run. Thus, from Eqs. (6)-(7) and the definition of τ ,

$$t_{1/2} \bar{R}_C = R_u \quad (8)$$

Therefore, we have obtained a simple relation which states that \bar{R}_C is inversely proportional to $t_{1/2}$ with R_u as the proportionality constant.

In the kinetic studies of coal gasification and pyrolysis, often the activation energy is estimated from an Arrhenius plot of initial reactivity R_{CO} , i.e., the reactivity at zero conversion, or half-life reactivity $R_{C,1/2}$, i.e., reactivity at 50% conversion. In some cases, rate constants k are obtained by fitting a model to the data, and activation energy estimated from an Arrhenius plot of the rate constants. Here, instead, let us define an average activation energy \bar{E}_C based on \bar{R}_C by the following Arrhenius relation:

$$\bar{R}_C = A \exp(-\bar{E}_C/RT) \quad (9)$$

This, when combined with Eq. (8), can be rearranged to get

$$t_{1/2} = (R_u/A) \exp(\bar{E}_C/RT) \quad (10)$$

Hence a plot of $\ln(t_{1/2})$ versus $(1/T)$ should yield a straight line with a slope equal to \bar{E}_C/R . In other words, Eq. (10) provides a simple means of estimating \bar{E}_C directly from the $t_{1/2}$ data alone.

EXPERIMENTAL

Kinetic studies of char-steam reaction of North Dakota lignite were conducted with a TGA apparatus (Peng et al., 1986) at pressures 1 atm and 7.8 atm, in the temperature range of 800 to 1200°C. The mean particle size of the coal sample was 178 microns and steam was in excess. The chars were generated "in-situ" by devolatilization in a steam-nitrogen atmosphere, and gasified in the same environment without interruption (Peng et al., 1986). The reaction was allowed to go to completion. The weight loss of the sample was continuously recorded on a microcomputer and analyzed. More details of our study will be available later (Raghunathan).

RESULTS AND DISCUSSION

Conversion versus time data were obtained for eleven gasification runs at both pressures. The data are plotted as x versus τ in Fig. 1 and the unification approach is seen to be valid for our data. For each of these runs, various two-parameter rate models from literature (Johnson, 1979; Simons, 1979; Bhatia & Perlmutter, 1980; Gavalas, 1980; Kasaoka et al., 1985) are fitted, and from the model that best fits the data, \bar{R}_C is calculated. Using those average reactivity data, we have plotted $(1/\bar{R}_C)$ versus $t_{1/2}$ in Fig. 2. Remarkably, they form a near perfect straight line passing through the origin with a correlation coefficient of 0.997 when fitted by the method of least squares, thus confirming the relation represented by Eq. (8). From the slope, the value of R_u is 0.385.

In Fig. 3, $\ln(t_{1/2})$ and $\ln(\bar{R}_C)$ are plotted versus $(1/T)$ for both pressures. At 1 atm, the plots are linear over the entire temperature range, and, when calculated from the slope, the \bar{R}_C values yield 61.1 kJ/mole for \bar{E}_C , whereas from the $t_{1/2}$ data, \bar{E}_C is 62.8 kJ/mole. Clearly the values are very close. For the same runs, Arrhenius plots of R_{CO} and $R_{C,1/2}$ yield activation energies of 64.5 and 60.8 kJ/mole, respectively.

For our experiments at 7.8 atm, the Arrhenius plot of average reactivity in Fig. 3 indicates the presence of two different controlling regimes: (1) between 1000°C and 1200°C, where the activation energy is nearly zero and (2) between 800°C and 1000°C, where a non-zero activation energy can be defined. The half-life data plotted in the same figure is seen to indicate this trend just as well. At this pressure, in the temperature range 800-1000°C, the \bar{R}_C values yield 43.6 kJ/mole for \bar{E}_C , and the $t_{1/2}$ values yield 43.0 kJ/mole. Again, the values are close. From the R_{CO} and $R_{C,1/2}$ values, the activation energies estimated are 44.4 and 43.5 kJ/mole, respectively. Discussions about the type of controlling mechanisms involved are beyond the scope of this article, and will be reported elsewhere.

Our results clearly indicate that, from the half-life data alone, (1) if there is a shift in the controlling mechanism in the temperature range, it can be detected by our method as well, and (2) the corresponding activation energy can also be estimated with reasonable accuracy.

Activation energy values are reported in literature for various gasification systems, evaluated through different methods. We have used the above approach to calculate the \bar{E}_c values from their half-life data alone and Table I shows the comparison. We did not test the validity of unification theory or Eq. (8) with their data, but the \bar{E}_c values so obtained are in good agreement with their reported values of activation energy. It is worth noting that the literature data shown in the table cover a wide variety of chars and represent different methods of estimating activation energy.

Hence, our results indicate that half-life data at different temperatures alone are sufficient to estimate the apparent activation energy of coal gasification reactions. This would eliminate the usually tedious and inaccurate procedures of evaluating the derivative of $x(t)$ associated with the estimation of reactivity and thus activation energy. Although experimental verification is based on coal gasification reactions, this method is expected to be applicable to other types of gas-solid reactions, e.g., oil shales retorting, and is certainly applicable to any reaction systems which satisfy the unification theory represented by Eqs. (3) and (4).

ACKNOWLEDGEMENT

This work was supported in part by the Department of Energy under Contract AC21-83MC20320. We thank I. C. Lee for helping with the experiments.

NOTATION

A	preexponential factor in Arrhenius relation
\bar{E}_c	average activation energy
$f'(\tau)$	$df(\tau)/d\tau$
k	rate constant
R_c	char reactivity
R_{c0}	initial reactivity
$R_{c,1/2}$	half-life reactivity
\bar{R}_c	average char reactivity
R_u	average normalized char reactivity, a universal constant

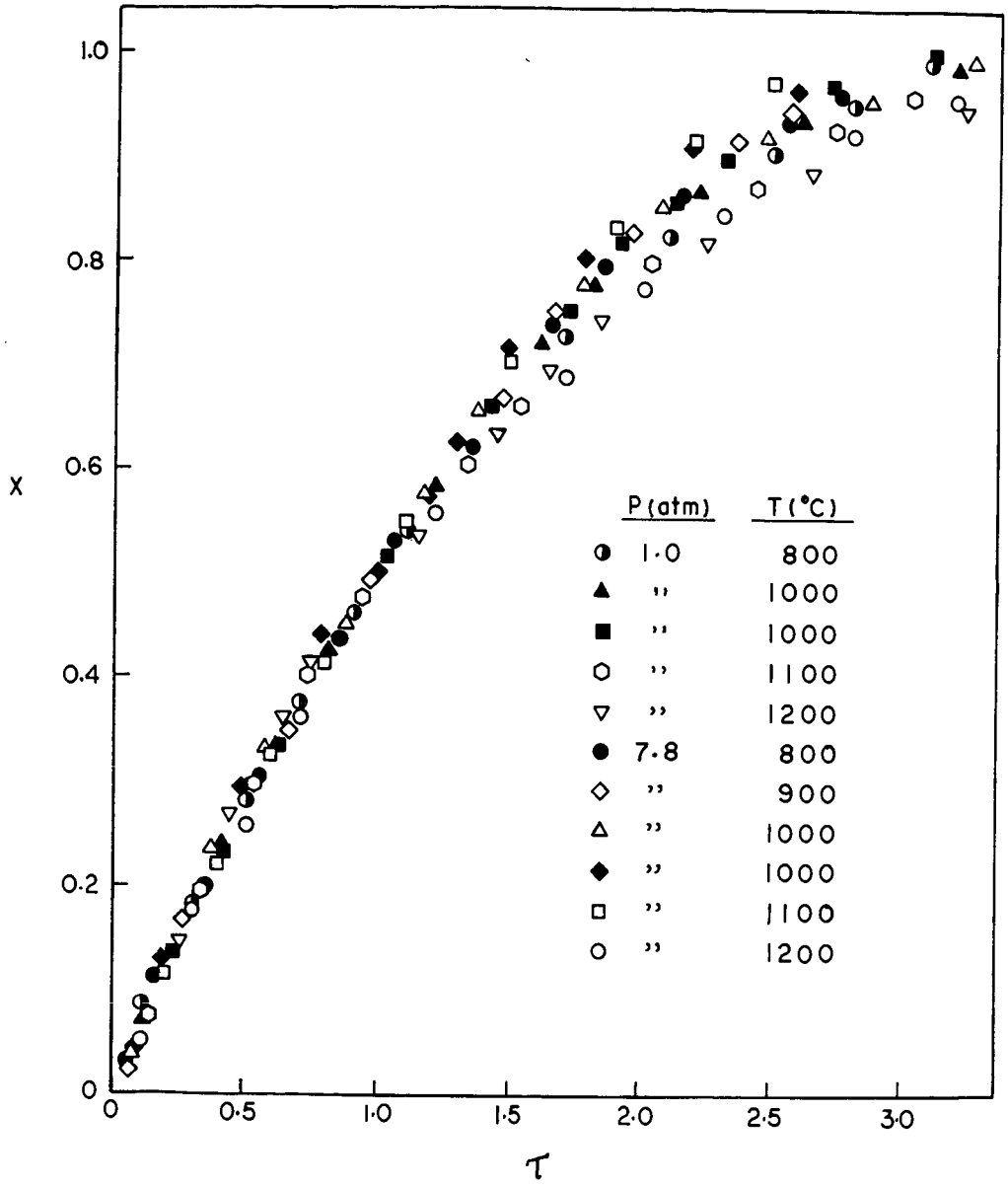
t	time
$t_{1/2}$	half-life of a reaction
T	reaction temperature
x	char conversion
τ	normalized time, $t/t_{1/2}$

LITERATURE CITED

- Bhatia, S. K., and Perlmutter, D. D., "A Random Pore Model for Fluid Solid Reactions: I. Isothermal, Kinetic Control," *AIChE J.*, 26, 379 (1980).
- Chin, G., S. Kmura, S. Tone, and T. Otake, "Gasification of Coal Char With Steam," *Int'l. Chem. Eng.*, 23, 105 (1983).
- Debelak, K. A., J. T. Malito, and R. M. Patrick, "Influence of Particle Structure on the Rate of Gas-Solid Gasification Reactions," *ACS Fuel Chemistry Division preprints*, 29, 82 (1984).
- Gavalas, G. R., "A Random Capillary Model with Application to Char Gasification at Chemically Controlled Rates," *AIChE J.*, 26, 577 (1980).
- Guzman, G. L., and F. E. Wolf, "Kinetics of K_2CO_3 -catalyzed Steam Gasification of Carbon and Coal, *Ind. Eng. Chem. Proc. Des. Dev.*, 21, 25 (1982).
- Johnson, J. L., "Kinetics of Coal Gasification", Wiley, 1979.
- Kasaoka, S., Y. Sakata, and C. Tong, "Kinetic Evaluation of the Reactivity of Various Coal Chars for Gasification with Carbon Dioxide in Comparison with Steam," *Int'l. Chem. Eng.*, 25, 160 (1985).
- Mahajan, O. P., P. L. Walker, Jr., and R. Yarzab, "Unification of Coal Char Gasification Reaction Mechanisms," *Fuel*, 57, 643 (1978).
- Peng, F. F., I. C. Lee, and R. Y. K. Yang, "Reactivities of In-situ and non-in-situ Coal Chars During Gasification in Steam at 1000 to 1400°C", *Proc. 3rd Pittsburgh Coal Conference*, 730 (1986).
- Raghunathan, K., Ph.D. Dissertation, West Virginia University, in progress.
- Schmal, M., J. L. F. Montelro, J. L. Castellan, "Kinetics of Coal Gasification," *Ind. Eng. Chem. Proc. Des. Dev.*, 21, 256 (1982).
- Schmal, M., J. L. F. Montelro, and H. Toscani, "Gasification of High Ash Content coals with Steam in a Semi-batch Fluidized Bed Reactor," *Ind. Eng. Chem. Proc. Des. Dev.*, 22, 563 (1983).
- Simons, G., "The Unified Coal-Char Reaction," *Fuel*, 59, 143 (1979).

Table 1

Source	Char	Medium	Activ. Energy (kJ/mol) from			
			R _{CO}	R _{C,1/2}	k	t _{1/2}
Our Data	lignite	steam	64.5	60.8	---	62.8
	lignite	steam	44.4	43.5	---	43.0
Peng et al. (1986)	bitum.	steam	56.8	36.5	---	43.9
	subbitum.	steam	60.6	57.2	---	61.7
	lignite	steam	84.7	79.7	---	91.1
	bitum.	steam	62.6	47.6	---	48.4
	subbitum.	steam	82.4	54.1	---	55.8
	lignite	steam	98.5	67.4	---	75.1
Debelak et al. (1984)	subbitum.	CO ₂	---	---	150.0	158.6
Chin et al. (1983)	brown coal activ. C	steam	---	---	125.6	129.4
	bitum. activ. C	steam	---	---	149.1	149.5
Schmal et al. (1982)	subbitum.	steam	---	---	165.4	161.6
Schmal et al. (1983)	subbitum.	steam	---	---	163.3	147.4
Guzman and Wolf (1982)	catalyzed activ. C	steam	---	---	259.6	250.7
	catalyzed bitum.	steam	---	---	242.8	239.8



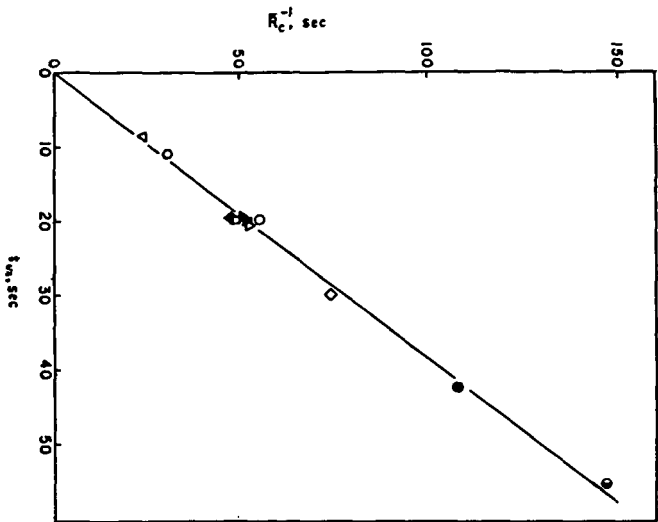


Figure 2. Reciprocal Average Reactivity versus Half-life

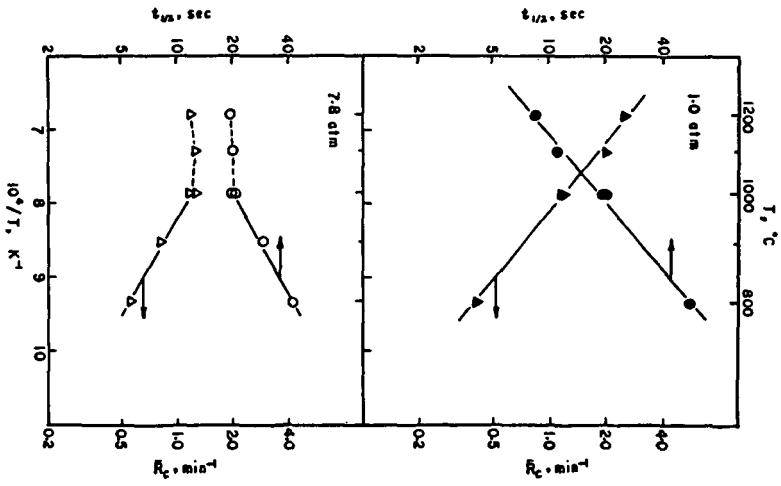


Figure 3. Comparison of Arrhenius Plots of Average Reactivity and Half-life at 1.0 and 7.8 atm.

**THE CHEMICAL BASIS FOR REMOVAL OF ORGANIC SULFUR
FROM COAL via JPL CHLORINOLYSIS**

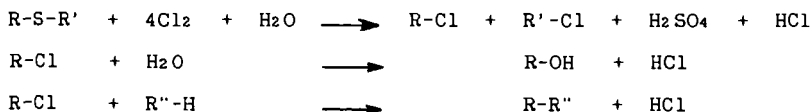
T. Aida, C. G. Venier, and T. G. Squires*

Ames Laboratory
Iowa State University
Ames, Iowa 50011

INTRODUCTION

Because of the environmental problems attributable to Acid Rain, sulfur removal has been one of the most important areas of coal utilization research. Although a number of physical and chemical desulfurization processes which effectively remove inorganic sulfur have been developed, only a small portion of the organic sulfur can be removed under these conditions (1). This is not surprising in view of the well established chemical stability of C-S bonds in thiophenes, arylsulfides, and thiophenols which comprise much of the organic sulfur component in coal.

While it seems obvious that investigation of the chemistry of coal desulfurization is necessary to develop more efficient and economical processes, this important research area has received little attention. For example, Chlorinolysis was investigated by the Jet Propulsion Laboratory more than ten years ago and reported to remove up to 60% of the organic sulfur (2). Yet the chemical pathway by which organic sulfur is removed is still unknown and is most often expressed with appropriate ambiguity in **Scheme 1** (3):

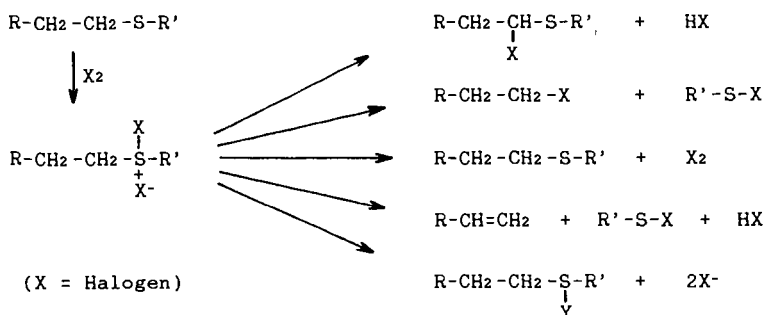


Scheme 1

However, the reactions of halogens with divalent sulfur compounds such as thiols, sulfides, and thiophenes have been studied extensively and are known to afford a complex product slate which is dependent on the specific halogen, the presence of nucleophiles, solvent, and temperature (4). In every case the reaction appears to proceed via initial formation of an intermediate halosulfonium salt. Established transformations from this species are shown in **Scheme 2**.

We have investigated the behavior of various organic sulfur functional groups under JPL Chlorinolysis conditions ($\text{Cl}_2/\text{CH}_2\text{CCl}_3/\text{H}_2\text{O}$) in order to elucidate the major desulfurization pathways. We have also looked at undesirable chlorination side reactions and have briefly examined conditions which minimize the ratio of chlorination to desulfurization.

* Present address: Associated Western Universities, Inc., 142 East 200 South, Suite 200, Salt Lake City, UT 84111.



Scheme 2

EXPERIMENTAL

General

Solvents and commercially available model organic sulfur compounds were used as received after checking their purity by gas chromatography. Di-*n*-butyltrisulfide was prepared by the reaction of *n*-butylthiol and thionyl chloride (4); and α -chlorosulfoxides were prepared by Tsuchihashi's method from the corresponding sulfoxide and sulfuryl chloride in the presence of pyridine (5). Gas chromatograms were run on a Varian 3700 using a 30 meter OV-101 fused silica capillary column; and yields were determined on the basis of internal standards. Products were identified by comparison of retention times and spectroscopic data with those of authentic samples. Sulfate analysis were performed by Ames Laboratory Analytical Services, ALAS. In order to minimize side reactions caused by excess chlorine, the reactions were carried out using the apparatus shown in Figure 1.

Chlorinolysis Procedure

The organic sulfur compound (6 mMol), dissolved in 60 mL of methylchloroform, was placed in the reaction flask with 30 mL of distilled water; and the vessel was immersed in a constant temperature bath. The reaction mixture was stirred and a gentle stream of nitrogen was bubbled through the mixture. Liquid chlorine (6mMol) was slowly vaporized into the nitrogen stream, and stirring and nitrogen bubbling were continued for a predetermined reaction time. After separating the layers, the aqueous layer was extracted with methylene chloride, and the combined organic extracts were analyzed by GC. Water was removed from the aqueous layer, and the residue was dissolved in methanol before treating it with diazomethane in ether. The resulting mixture was analyzed for methyl sulfonates by GC.

RESULTS & DISCUSSION

Our initial experiments were designed to identify discrete intermediates in the desulfurization pathway. Consequently, reactions were carried out at low temperatures using an apparatus (Figure 1) capable of precise control of chlorine addition. The results from these experiments are shown in Table 1.

Table 1. JPL Chlorinolysis of Coal Model Organic Sulfur Compounds.

Starting Material	Cl ₂ (Equiv)	Temp (°C)	Time (Hr)	Products (%)	
Ph-S-Ph	1.0	0	0.5	Ph-S-Ph (92)	Ph-S(=O)-Ph (5)
	3.0	25	2.0	O (Tr)	O (93)
Dibenzothiophene	1.0	0	0.5	Sulfoxide (90)	Sulfone (7)
	3.0	25	2.0	(Tr)	(96)
Ph-S-H	2.0	0	0.5	Ph-S-Cl (70)	Ph-SO ₃ H (13)
	3.0	25	2.0	O (0)	(93)
Bu-S-Bu	1.0	0	0.5	Bu-S-Bu (41) ^a	Bu-S-CH-Pr (20)
	3.0	25	2.0	O (0) ^b	O Cl (0)
Dimethylthiophene	1.0	0	0.5	No products detected by GC	
	2.0	25	2.0	No products detected by GC	

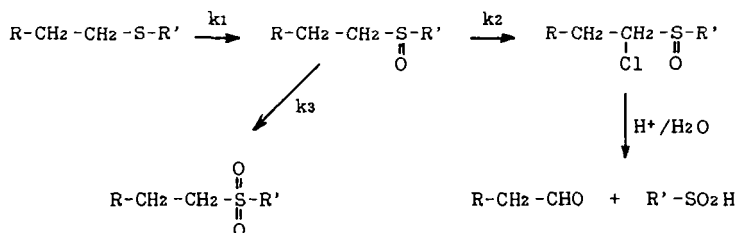
^a 30% Starting Material remaining.

^b No Starting Material detected.

As previously reported (5), the reaction of chlorine with phenyl sulfide and dibenzothiophene proceeds via consecutive oxidation at sulfur. Under mild conditions (0°C, 30 min., 1 equiv Cl₂) the sulfoxides were obtained in very high yields (>90%) compared to reactions carried out under ambient conditions (6). Extensive amounts of sulfones are produced under the latter conditions. Similarly, benzenethiol was converted to the corresponding sulfinyl chloride in substantial yield (70%) under mild conditions and quantitatively to benzenesulfonic acid under slightly more severe conditions.

In the case of *n*-butylsulfide, the reaction mixture was complex and highly dependent on reaction conditions, suggesting the involvement of consecutive multi-step reaction pathways. This reaction was examined more closely by cooling the reaction mixture to 0°C and slowly (2 min.) adding chlorine in 0.5 equivalent aliquots at 5 minute intervals. Samples of the reaction mixture were withdrawn for analysis just prior to the introduction of each aliquot of chlorine, and the results are plotted in Figure 2. Only trace amounts of *n*-butylsulfone were detected in the reaction mixture. In a separate experiment, when an equimolar mixture of *n*-butylsulfide, -sulfoxide, and -sulfone was reacted with excess chlorine, only the sulfone (80%) was recovered.

In fact, α -chlorination of alkylsulfoxides is a well established reaction (7); and it is also known that under acidic conditions, α -chlorosulfoxides are readily hydrolyzed, proceeding via carbon-sulfur bond scission to afford the corresponding aldehyde and sulfinic acid (8). In conjunction with this information, our experiments provide clear evidence for the intermediacy of the α -chlorosulfoxide as shown in reaction Scheme 3.



($k_1 > k_2 \gg k_3$)

Scheme 3

In order to determine whether α -chlorosulfoxides can be hydrolyzed under JPL Chlorinolysis conditions, α -chlorosulfoxides were prepared and subjected to standard reaction conditions with excess chlorine at ambient temperature for two hours. The results are shown in Table 2; in both cases, the labile C-S bond was cleaved under these mild conditions. These observations provide additional support for Scheme 3 as a desulfurization pathway.

Table 2. JPL Chlorinolysis of α -Chlorosulfoxides.

Starting Material	Product (%)
$ \begin{array}{c} \text{Bu-S-CH-C}_3\text{H}_7 \\ \parallel \quad \\ \text{O} \quad \text{Cl} \end{array} $	Bu-SO ₃ H (76)
$ \begin{array}{c} \text{Ph-S-CH}_2\text{-Cl} \\ \parallel \\ \text{O} \end{array} $	Ph-SO ₃ H (94)

A final set of experiments were performed to provide additional information about the fate of sulfur functionalities under JPL Chlorinolysis conditions. The sulfate ion concentration was determined in the reaction mixtures of a series of coal model organic sulfur compounds. The results, given in Table 3, clearly reveal significant limitations concerning the type of C-S bonds that can be cleaved. Specifically, C-S bonds undoubtedly survive intact in aryl thiol, diaryl sulfide, and dibenzothiophene systems even though the sulfur itself is oxidized. On the other hand, dialkyl sulfides, thiophenes, and perhaps alkyl thiols appear to be susceptible to significant desulfurization.

It is particularly interesting that polysulfides, including elemental sulfur, are desulfurized almost quantitatively. While the concentration of polysulfides has not been established for a wide range of coals, it appears to be significant in some coals. For example, polysulfides were found to comprise 20% of the sulfur in a pyridine extract of Western Kentucky No. 9 coal (9). The wide range

of sulfur removal reported by JPL (1) may reflect not only differences in rank but also differences in the concentration of labile organic sulfur functional groups such as polysulfides.

Table 3. Yields of SO₄ from JPL Chlorinolysis Reaction Mixtures.^a

Starting Material	SO ₄ (%) ^b
Diphenyl Sulfide	0
Dibenzothiophene	0
Thianaphthene	0
Thiophenol	0
2,5-Dimethylthiophene	12
Dibutyl Sulfide	38
Dibutyl Trisulfide	94
Sulfur	98

^a Excess Cl₂, 50°C, 1 hour.

^b Based on sulfur.

REFERENCES

1. Morrison, G.F. "Chemical Desulfurization of Coal", IEA Coal Research Report No. ICTIS/TR15, London, 1981.
2. Kalvinskis, J.; Grohman, K.; Rohatgi, N.; Ernest, J.; Feller, D., JPL Final Report, Phase II, "Coal Desulfurization by Low Temperature Chlorinolysis", 1980.
3. Vasilakos, N.P.; Corcoran, W.H. Fuel 1983, 62, 1111.
4. Wilson, G.E. Tetrahedron 1982, 38, 2625.
5. Squires, T.G.; Venier, C.G.; Goure, W.F.; Chang, L.W.; Shei, J.C.; Chen, Y.-Y.; Hussman, G.P.; Barton, T.J. "The Use of Model Organosulfur Materials to Investigate the Chemical Desulfurization of Coal" presented to the AIChE at Chicago, November 1980.
6. Chapter 8 in "Organic Chemistry of Sulfur", Oae, S., ed., Plenum Press, New York, 1977.
7. Tsuchihashi, G.; Ogura, K. Bull. Chem. Soc. Japan 1971, 44, 1726.
8. Oae, S., personal communication.
9. Hurd, C.D. Quart. Rep. Sulfur Chem. 1965, 4, 75.
10. Aida, T., unpublished results.
11. Richtzenhaim, H.; Alfredsson, B.; Ber. 1953, 86, 142.
12. Field, L.; Laceyfield, W.B. J. Org. Chem. 1966, 31, 3555.

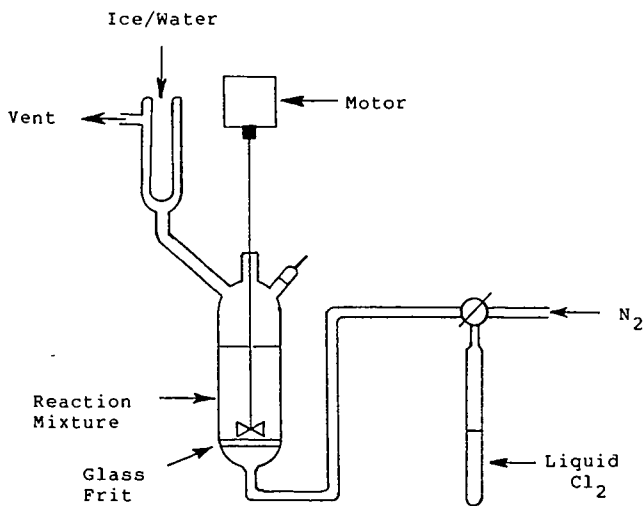


Figure 1. Chlorination Apparatus

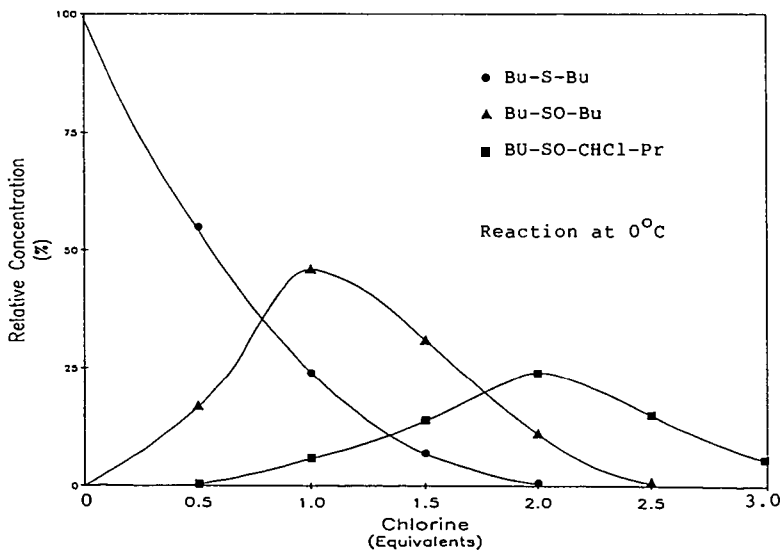


Figure 2. Chlorinolysis of Di-n-butyl Sulfide

THE EIGHT COALS
IN THE
ARGONNE PREMIUM COAL SAMPLE PROGRAM*
Karl S. Vorres and Stuart K. Janikowski

Chemistry Division
Argonne National Laboratory
9700 S. Cass Ave.
Argonne, IL 60439

* Work performed under the auspices of the Office of Basic Energy Sciences, Division of Chemical Sciences, U. S. Department of Energy, under contract number W-31-109-ENG-38.

ABSTRACT

The full set of eight coals for the Premium Coal Sample Program includes a lignite, subbituminous, high volatile, medium volatile and low volatile bituminous, as well as a resinite rich, an inertinite rich and a Pittsburgh #8 coking coal. The coals were selected on the basis of C, H, S and O content as well as maceral content and geological age. Ampoules are typically available in 5 grams of -100 mesh or 10 grams of -20 mesh material. Some analytical information is available. The methods of selection, collection, transportation, processing, packaging, distribution and characterization are summarized.

INTRODUCTION

The Premium Coal Sample Program is intended to provide the basic coal research community with the best quality samples of a limited number (8) of coals for basic research. The availability of the ampoules is the result of the cooperation of many individuals within a number of organizations whose efforts made the high quality of the samples possible.

The premium coal samples produced from each coal and distributed through this program are chemically and physically as identical as possible, have well characterized chemical and physical properties, and will be stable over long periods of time. Coals have been mined, transported, processed into the desired particle and sample sizes and packaged in humid nitrogen environments as free of oxygen as possible. The need for a Premium Coal Sample Program was expressed at the Coal Sample Bank Workshop held March 27 and 28, 1981 in Atlanta, Georgia.

SELECTION OF THE COALS

Support has been provided by the Office of Basic Energy Sciences to make eight carefully selected coals available. The selection of these coals was based on those parameters which would represent significant differences among the available coals and maximize our understanding of the fundamental properties of coal. A cluster analysis was carried out to establish desirable samples in terms of the significant compositional parameters, C, H, O and S. Paul Neill used data from the Penn State data base on over 200 coals which had been described as representing channel ranks and compositions. The cluster analysis resulted, using increasing carbon and decreasing oxygen on one axis and hydrogen and sulfur content on the other, in identification of compositional characteristics for eight coal samples. These were used to indicate a set of initial sample choices.

The sample characteristics from the cluster analysis are indicated in Table I.

Table I. The Composition Characteristics of The Eight Coals Selected in the Cluster Analysis.^{a,b} (Moisture, ash-free basis)

Group	% Carbon	% Hydrogen	% Sulfur	% Oxygen
1	73.6 (1.5)	4.9 (.2)	0.5 (.2)	20.0 (1.5)
2	74.5 (1.9)	5.6 (.5)	1.1 (.4)	17.5 (2.0)
3	79.0 (1.7)	5.5 (.4)	4.4 (.3)	10.0 (1.5)
4	79.2 (2.0)	5.6 (.4)	0.9 (.6)	12.8 (2.0)
5	82.7 (2.0)	5.7 (.4)	1.3 (.6)	8.1 (1.8)
6	85.4 (1.4)	5.4 (.3)	0.8 (.3)	6.8 (1.4)
7	89.6 (1.0)	4.9 (.3)	0.8 (.3)	3.2 (1.0)
8	91.3 (0.5)	4.3 (.2)	0.7 (.2)	2.3 (0.6)

a) Oxygen is by difference

b) Values in () represent + or - values.

The list was then examined to consider the variety of maceral contents which exist in U. S. coals. There are three important maceral types, vitrinite, liptinite and inertinite. Vitrinite is the major maceral type in U. S. coals, accounting for about 85% of the total. Liptinites are hydrogen-rich macerals and inertinites are hydrogen deficient. Variations in hydrogen content can be achieved by seeking coal samples rich in certain of the liptinites or inertinites. The liptinites include resinite, from the waxy parts of plants, and sporinite derived from plant spores.

With help from the U. S. Geological Survey, individual coals were identified for collection. Details of the samples are given at the end of this paper. Samples #1,2,3,5 and 8 were selected to give a range of compositional parameters, primarily carbon,

hydrogen and oxygen which vary with the degree of coalification of the sample. In addition #3 was selected to provide the sample with a relatively high sulfur content. Coal #4 was also selected for its known coking properties, coal #6 was selected for high resinite and #7 for sporinite and inertinite contents.

COLLECTION OF THE COALS

The collection of coal samples began by identifying the potential sources of coal samples and seeking permission to acquire the samples. The U. S. Geological Survey provided at least one staff geologist at each site for supervision of the actual collection of the sample and to document the seam for later description in USGS Circulars to provide a permanent, referenceable description of the sample.

For a typical underground sample, the mine operator met with the USGS, sample collection crew, truck driver and Program Manager in advance of the sample collection to discuss details of the collection. On the morning of the collection, the coal seam face was freshly exposed to provide a block of coal the thickness of the coal seam, about one foot wide and long enough to provide for the one ton sample. The seam was exposed with a continuous miner, and a roof bolter immediately followed to secure the seam roof. The loose coal was scraped away from the sample block, and several layers of plastic sheets were placed on the mine floor. After measuring and calculating the amount needed for the sample, the block was marked by the USGS representative. The sample was then removed by the collection crew with hand picks from the roof to the floor to provide a channel type sample. Partings over an inch thick were discarded. Particular care was taken to avoid contamination of the sample with material nearby. When the seam thickness exceeded four feet, stainless steel drums were taken into the mine for sample collection. Alternatively, double plastic bags were used to transport the coal to the surface. In all cases, the coals were loaded into stainless steel drums from 1/2 to 5 hours after collection and then purged with argon.

The subbituminous sample was collected as a 6" core sample from the Wyodak seam that was about 120' thick at the sample site. The drilling contractor also obtained two additional 3" cores, one for the USGS, and the other for long term storage of the sample. All cores were rinsed with distilled, deaerated water immediately after they were released from the core barrel and loaded into the stainless steel drums for shipment.

The lignite sample was obtained as a series of 3" core-type samples drilled through the seam at about 20' intervals over a freshly exposed top surface. Cold weather limited reactions at the surface. This approach provided channel type samples representative of a sample area of about one acre. The samples were also quickly loaded into the drums and purged.

TRANSPORTATION OF THE SAMPLE

The samples were always moved in the same truck which was operated by the same driver. The truck was loaded with stainless steel drums, argon cylinders and tools at ANL and then driven to the mine site. The drums were usually loaded on the truck with a forklift. The samples were purged with 99.999% argon gas using a calculated volume to reduce the oxygen concentration to below 100 ppm. The sealed drums were pressurized to about 6 psig and then transported in a refrigerated semi-trailer at temperatures of 40-45 F to prevent freezing and limit chemical reactions on the way to the processing facility at ANL. The samples arrived at the laboratory within one-half to two days of the purging, and were immediately unloaded.

PROCESSING OF THE SAMPLES

After the stainless steel drums were unloaded from the truck, they were weighed, recorded and transferred to the first airlock in the nitrogen filled processing facility. This facility is a large enclosure in two parts, each of which was constructed of sheets of aluminum and plastic windows. Seventy pairs of long rubber gloves mounted in the windows permit manipulation of the samples and equipment during the processing. The dimensions of the facility are about 5-6' wide, 13' high and the equivalent of 40' long. The two parts are separated by a sealed mixer-blender. The oxygen concentration in the facility was maintained below 100 ppm during processing of the samples. Oxygen control is part of the gas handling system design which includes a cyclone separator, high efficiency particulate filter, industrial blower and cooling coils as well as steam supply for humidity control. A part of the gas stream is passed over a palladium on alumina catalyst with a slow stream of hydrogen to react with and convert the trace amounts of oxygen to steam.

After the first airlock containing the coal drums was purged with nitrogen to less than 100 ppm oxygen, as established by analysis of the gas by the fuel cell analyzer, the drum lids were removed. The drums were moved to the hydraulic drum dumper and fastened in place. The contents of the drum were dumped into a crusher which reduced the coal particles to a size such that one dimension was no more than 1/2". The crusher discharge flowed down a chute with a variable gate to control the flow rate to a Syntron vibratory lift which raised the crushed coal to the top of the enclosure. A pulverizer feeder controlled the rate of flow to the pulverizer, which has a nominal capacity of 300 pounds per hour. Initially a 20 mesh screen was used with the hammer mill. The pulverized coal flowed down into the mixer blender which has a 2000 liter capacity, and can hold the entire one ton sample. The sample was accumulated and then thoroughly mixed in the blender. Earlier studies at the vendor's facility demonstrated that mixing was achieved in less than four minutes.

PACKAGING OF THE SAMPLES

The thoroughly mixed sample was then conveyed by means of a tubular conveyor to a filling station for five gallon "leverlock" pails or borosilicate carboys. One half of the batch was transferred in the five gallon pails back through airlocks for further pulverizing to pass a 100 mesh screen. The balance of the -20 mesh material was transferred to ampoule filling and sealing equipment. Ten grams of -20 mesh or five grams of -100 mesh material (except for the Wyoming sample) were dispensed into amber borosilicate ampoules. The ampoules were sealed with a hydrogen-oxygen flame. The gas supply was controlled with two gas mass flow controllers and set to provide for stoichiometric combustion. The oxygen levels do not change in the box due to torch operation. The sealed ampoules were removed through airlocks and then placed in storage.

STORAGE

The samples and borosilicate carboys are kept in racks in a dark room that is kept close to 72°F year round. The borosilicate carboys can be used to replenish supplies of the ampoules whenever needed to sustain the inventory for shipments. It is expected that about 75,000 ampoules can be provided from each sample. This quantity of ampoules can meet requests for 30 ampoules per day for the next decade and is expected to meet the needs for a substantially longer period.

DISTRIBUTION OF THE SAMPLES

Product announcements are sent out to a mailing list of individuals who have asked to be included or are active in basic coal research. Orders are placed through the Assistant Controller at ANL, and are sent to the Program Manager for filling. Each ampoule is inspected before being placed in special cardboard cartons for shipping. These cartons have foam bottom and top layers, and partitions to provide for space between the ampoules and the wall of the carton for added protection. Samples are typically sent by United Parcel Service (UPS).

Each researcher is asked to provide a short statement of the nature of the work, such as molecular structure studies by pyrolysis-mass spectrometry, so that an understanding of the different types of research activity may be obtained for the overall program. In addition the researcher is asked to provide references to public domain documents such that a bibliography of research with the samples can be made available to all researchers to further the progress of basic coal science. This bibliographic information will become available in either a printed version or through a dial-up modem.

Samples are available in 5 grams of -100 mesh or 10 grams of -20 mesh material for the first seven coals except for the Wyodak sample which is only available in the -20 mesh size. The eighth sample should become available in April 1987.

CHARACTERIZATION OF THE SAMPLES

The coal samples are being characterized for three purposes: establishing the homogeneity of the samples, characterizing the samples physically and chemically, and monitoring the stability of the samples in storage. The homogeneity of the samples was evaluated using 39 samples taken during the course of the packaging and submitting them for irradiation at the University of Illinois TRIGA reactor. The three or four most suitable radioisotopes that were produced were then counted over a period of two weeks to establish the activity per unit of mass and then compared to examine variation and trends. The characterization consisted of an analysis for a range of chemical and physical properties by up to 70 different laboratories. The list of chemical and physical analyses is given below:

Chemical analyses:

- Ultimate, C, H, S, N, O (by difference)
- Proximate: moisture, ash, volatile matter, fixed carbon
- Major and minor elements in the ash
- Equilibrium moisture
- Direct oxygen by fast neutron activation

Physical measurements and analyses:

- Petrographic
- Maceral analysis
- Ash fusion temperatures
- Gieseler plasticity

The stability in storage has been evaluated in several ways. For bituminous coals the Gieseler plasticity has been measured periodically. For all coals the gas atmosphere over the samples has been analyzed periodically.

DESCRIPTION OF THE SAMPLES

1. The first is an Upper Freeport seam medium volatile bituminous sample collected near Homer City, Pennsylvania (Indiana County) in January 1985. The seam was 4' thick at the collection point. Sample characterization provides the following values (prelim. as received basis):

carbon:	75.7%	ash:	13.1%
hydrogen:	4.82%	moisture:	0.85%
total sulfur:	2.42%		

2. The second sample is from the Wyodak seam, a subbituminous coal collected about 6 miles northeast of Gillette, Wyoming (Campbell County) in October, 1985. The seam was about 120' feet thick at the collection site. The sample for processing consisted of a 6" core sample through the entire seam. The preliminary analysis of the sample on an as-received basis is:

carbon:	65.4%	moisture:	28.7%
hydrogen:	5.18%	ash:	9.8%
sulfur:	0.66%		

Due to the high moisture content of this sample it is being offered only in the ampoules containing 10 grams of -20 mesh.

3. The third sample is a high volatile bituminous coal, from the Illinois #6 or Herrin seam, and was collected about 60 miles southeast of St. Louis (St. Clair county) in December, 1985. The 55 gallon drums were taken into the mine since the seam was about 7' thick at the collection site. The preliminary analytical values, on a dry basis (except moisture) are:

carbon:	65.2%	moisture:	8.8%
hydrogen:	4.82%	ash:	16.2%
sulfur:	4.6%		

4. The fourth coal, a Pittsburgh #8 seam, was collected about 60 miles south and west of Pittsburgh in Greene County, Pennsylvania in March 1986. This seam was about 6' thick at the collection site. The sample drums were again taken into the mine to facilitate the loading of the drums at the surface. The preliminary analytical data on an as-received basis (in %) follow:

carbon:	75.6	moisture:	1.8
hydrogen:	5.34	ash:	9.3
total sulfur:	2.1		

5. The fifth sample is a low volatile bituminous from the Pocahontas #3 seam, collected in Buchanan County, Virginia in June, 1986. The seam was about 6' thick at the collection site, and the drums were taken into the mine. The preliminary analytical data on an as-received (in %) basis are:

carbon:	85.4	moisture:	0.7
hydrogen:	4.5	ash:	4.9
total sulfur:	0.6		

6. The sixth sample is a Utah Blind Canyon seam sample collected in Emery County about 150 miles south and east of Salt Lake City, Utah. The seam was about 7' thick at the collection site. Some preliminary analytical data on an as-received basis are:

carbon:	74.1%	hydrogen	5.7%	resinite	11%
---------	-------	----------	------	----------	-----

7. The seventh sample is from the Lewiston-Stockton seam of the Kanawha formation, collected about 20 miles east of Charleston, West Virginia (Kanawha County). The seam was about 6' thick at the collection site. Preliminary data indicate that this sample contains about 73% vitrinite, 16% inertinite and 11% exinites, almost all of which is sporinite, 65.1% carbon and 4.38% hydrogen.

8. The eighth sample is from the Beulah-Zap seam collected in Mercer county, North Dakota about 8 miles northwest of Beulah. The seam was about 18 feet thick at the collection site. Collection was done by accumulating about 50 of 3" sample cores spaced about 20' apart in each direction. These were immediately loaded into the drums.

ADVISORY BOARD

A group of seven prominent coal researchers is involved with the Program in an advisory capacity to provide the Program Manager with advice and counsel on a range of issues. These people met on an annual basis and also provided advice informally at other meetings and through phone conversations. Those serving at present and in the past include: C. Blaine Cecil, USGS; John Larsen, Lehigh University; Marvin Poutsma, ORNL, Ronald Pugmire, University of Utah; William Spackman, Pennsylvania State University; Leon Stock, University of Chicago; Irving Wender, University of Pittsburgh; Randall Winans, Argonne National Laboratory, John Young, Argonne National Laboratory

ACKNOWLEDGMENTS

The author gratefully acknowledges the support from the Office of Basic Energy Sciences, Chemical Sciences Division which makes the program possible, the contributions from each of the eight mine owners and operators for both the time of the personnel and the coal itself, and the Advisory Board for their many helpful comments and suggestions. The efforts of each of the many individuals at the USGS, Pittsburgh Testing Inspectorate, Randy Engelhart, the truck driver, and the many individuals who designed, built and operated the facility, and Joe Gregar, the glassblower who sealed the glass carboys, and other individuals at ANL who made the program possible there is also appreciated.

THE RELATIONSHIP BETWEEN
CATION MOBILITY AND ACID-BASE BEHAVIOR
IN COAL ASH AND SIMILAR OXIDE SYSTEMS

Karl S. Vorres

Chemistry Division
Argonne National Laboratory
Argonne, IL 60439

ABSTRACT

Acids and bases were defined earlier in terms of the ionic potential or cationic charge/radius ratio. Values range from about 10 for acids to about 1 for bases when crystallographic radii in Angstrom units are used. The ionic potential reflects the relative attraction of a cation for charges on a uniform anionic surface. Surface cations have different mobilities on a common anion surface. The most basic ions have the greatest mobility due to the relatively weak attraction for surface anions, which minimizes the energy requirement for surface diffusion and leads to an enhancement of sintering.

INTRODUCTION

The physical properties of mixtures depend on the chemical composition of the constituents. In coal, the mineral matter is a mixture of mineral species. These minerals have been formed from cationic and anionic constituents of widely differing charge and radius. The different charges and sizes lead to different acid-base behavior for the mineral matter. Earlier the ionic charge and radius was used to develop a scale of ionic potential (ionic charge/crystallographic radius of the cation) values for comparing behavior and properties (1,2) of coal ash and similar oxide systems. This scale has been used to interpret the viscosity behavior of molten coal ash (3), and can be used as a guide to selection of additives for modifying the melting behavior of ash.

MINERAL MATTER SOFTENING AND MELTING

The mineral matter in coal is usually a mixture of relatively high-melting species. On heating the interactions between these species takes place slowly and sometimes produces glassy phases. As a result, coal ash and mineral matter samples do not exhibit sharp melting points. The ASTM procedures for reporting ash soft-

tening and melting behavior reflect this behavior (4).

The relatively slow reactions are attributed to the time requirements to bring the reactants together and for the reaction to form new phases. For the relatively silica-rich phases there is relatively little of the mobile species to diffuse rapidly.

ACID AND BASE BEHAVIOR

The thermal behavior of coal ash has been described in terms of the melting, viscosity, fouling and slagging. The latter two terms refer to the accumulation of ash material on tubes or wall of boilers. Correlations have been made of ash melting behavior with compositional parameters including silica ratio, dolomite percentage, ferric percentage, sodium content, base content and base-to-acid ratio (5,6,7,8).

In earlier correlations, acids were defined as oxides of Al, Si, and Ti, while bases were defined as oxides of Na, K, Ca, Mg and Fe (6). Other species were not defined, and oxidation states were not involved in the definition, other than to refer to the form of the oxide commonly reported in the analysis. The behavior as an acid or base is related to the structural inorganic characteristics of the ions involved. The inorganic cations may be ranked according to their size or ionic radii for their common valences. In general, ionic radii decrease with increasing cationic charge and also decrease with increasing atomic weight for a given valence.

Values for the cation radii selected from a set given by Ahrens (9) for the metals indicated above are listed below in Angstrom units:

ion	radius	ion	radius
Si ⁺⁴	0.42	Fe ⁺²	0.74
Al ⁺³	0.51	Na ⁺¹	0.94
Fe ⁺³	0.64	Ca ⁺²	0.99
Mg ⁺²	0.67	K ⁺¹	1.33
Ti ⁺⁴	0.68		

The two values for iron are given to indicate that each is important and that the behavior of iron compounds is affected by the oxidation state, which is in turn governed by the gaseous environment and temperature.

IONIC POTENTIALS

Another structural concept is that of ionic potential. The ionic

potential is defined as the quotient of the valence or cationic charge and the cationic radius for a given cation. This parameter is a measure of the electrostatic attraction or ability of a given cation to compete with other cations around it for coordinating a common anion, such as the oxide ion. A high value of the ionic potential indicates a strong ability to compete effectively with other cations to form some coordinated complex. Conversely a low value indicates a weak electrostatic attraction or poor ability to compete to form a complex. Therefore a relatively small amount of energy would be required to dislodge the cation from a given complex or site on a surface. The values of the ionic potentials from the cation radii, in Angstrom units, indicated earlier and the oxidation states of the the species of interest are indicated below:

ion	ionic potential	ion	ionic potential
Si ⁺⁴	9.5	Fe ⁺²	2.7
Al ⁺³	5.9	Ca ⁺²	2.0
Ti ⁺⁴	5.9	Na ⁺¹	1.1
Fe ⁺³	4.7	K ⁺¹	0.75
Mg ⁺²			

The highest values belong to the acid group of Si, Al and Ti while the lowest values are associated with the bases K, Na, Ca and also ferrous iron. This scale is useful in understanding and quantifying acid and base behavior.

SURFACE DIFFUSION

Other properties also depend on the ionic potential parameters. One of them is surface diffusion. The structure of an idealized solid oxide surface is an ordered array of sites occupied by anions (oxide ions) and a variety of cations. Diffusion across the surface depends on the availability of enough energy to move a surface species from one site to an adjacent site. The energy requirements for a system which can be considered primarily in terms of ionic bonding are a function of the electrostatic forces between the surface substrate and the mobile surface species. In coal ash or mineral species the predominant anion is the oxide ion. To a first approximation, the surface can be considered as a set of oxide anions arranged at sites whose locations and distances apart are a function of the associated cations. Surface cations will be attracted to anionic sites by electrostatic forces, particularly so for the more ionic species characterized by low charge and large radii. These properties are also used to characterize bases on the the ionic potential scale. The energy required to move an ion from one site to an adjacent similar site is largely determined by the magnitude of the ionic potential of

the ion. Therefore those ions with the lower ionic potential will move more easily, or for a given amount of thermal energy, a larger fraction of the ions with the lower ionic potential will migrate from the original sites to adjacent and other ones in a given amount of time.

For two adjacent particles with somewhat different chemical compositions, such as coal mineral matter or ash particles, the ions with the higher mobility or lower ionic potential will preferentially migrate to other particles with the smaller concentration of these ions. As a result the surface of the other particles will be coated with a lower melting phase than would have been possible from the interaction of the species within the higher melting particle. This process will continue at a rate dependent on the supply of low ionic potential ions from the original particle, bulk diffusion of the ions and thermodynamic equilibria.

The diffusion of low ionic potential particles is likely to be much more rapid across surface (by an order of magnitude) than bulk diffusion due to the relative ease when attracted on only one side, and the lack of need to tunnel into the relatively solid oxide structure or to find pores within it. The relatively larger size of these ions also limits the bulk diffusion rate. The result of rapid surface diffusion is "fluxing" or formation of lower melting phases which contribute to the sintering of two or more adjacent particles.

ACKNOWLEDGMENTS

The author expresses appreciation to the U. S. Department of Energy, Office of Basic Energy Sciences, Chemical Sciences Division, whose support made this work possible.

REFERENCES

1. Vorres, K. S., Am. Chem. Soc., Fuel Chem. Div., 22, (4) 118 (1977)
2. Vorres, K. S., in "Analytical Methods for Coal and Coal Products", edited by Karr Jr., C., Academic Press, Inc. (1979), Chap. 53, pp.481 ff
3. Vorres, K. S., Greenberg, S., and Poeppe, proc. Second Intl. Conf. Metallurgical Slags and Fluxes, 1984, The Metallurgical Society of AIME, Nov. 1984, ed. by H. A. Fine and D. R. Gaskell.
4. ASTM, 1977 Annual Book of ASTM Standards. Part 26: Gaseous

Fuels; Coal and Coke: Atmospheric Analysis," p. 266. ASTM, Philadelphia, Pennsylvania.

5. Winegartner, E. C. and Rhodes, B. T. J. Eng. Power, 97, 395 (1975)

6. Bryers, R. W. and Taylor, T. E. Amer. Soc. Mech. Eng.. Pap. 75-WA/CD-3.

7. Sage, W. L. and McIlroy, J. B., J. Eng. Power, 82, 145(1960).

8. Babcock and Wilcox Co., "Steam - Its Generation and Use", Chap. 15, (1978) Babcock and Wilcox Co., New York, New York

9. Ahrens. L. H., Geochim. Cosmochim. Acta 2, 155 (1952).

ADSORPTION OF SULFUR DIOXIDE FROM COMBUSTION GASES
ON A REGENERABLE MOLECULAR SIEVE

Colin Chriswell and Sai Gollakota

Ames Laboratory, Iowa State University, Ames, Iowa 50011

ABSTRACT

A new molecular sieve adsorption process is being developed for removal and recovery of sulfur dioxide from combustion gases. Desirable features of the process include:

- SO₂ accumulation is efficient at temperatures ranging from 50°C to >800°C, at pressures ranging from 1 to 30 atmospheres, and at SO₂ concentrations ranging from 500 ppm to 100%.
- Rates of adsorption are high, bed depth requirements are low, and back pressures are negligible.
- Sulfur dioxide is selectively adsorbed in the presence of major and trace constituents of combustion gases.
- Preliminary evaluation indicate the process will be competitive in costs with wet-lime scrubbing, but also it will be applicable to hot combustion gases that cannot be desulfurized by existing methods.

INTRODUCTION

Well-established, effective, but costly processes exist for flue gas desulfurization. Installation of wet-lime scrubbers on new coal-fired electric plants contribute about 15% to construction costs and consume about 4% of energy inputs to the plant (1). Less expensive alternatives are desirable, but because of the high cost involved, only well-proven techniques are considered for flue gas desulfurization.

Direct coal-fired gas turbines can produce electricity more economically than steam plants (2). Cleanup of high-temperature, high-pressure gases entering turbines is needed to prolong turbine life as well as to meet environmental requirements. Viable processes do not exist for removal of sulfur dioxide from gases at temperatures greater than 1000°F (550°C) and at pressures greater than 10 atmospheres.

During the 1960's, the U. S. Bureau of Mines demonstrated that sulfur dioxide could be removed from flue gases and recovered using molecular sieve adsorbents (3, 4). Union Carbide subsequently developed and commercialized a process called Purasieve S which used molecular sieves for recovering sulfur dioxide from gas streams (5). At temperatures of flue gases (100°-200°C) the molecular sieve processes were effective, capital and operating costs were low, and high-purity sulfur dioxide was recovered as a by-product. However, the processes were not accepted. Attrition rates for the relatively costly molecular sieves were too high. Their alumina skeletons were degraded by corrosive agents in the gas streams.

In 1978, Flanigan and co-workers at Union Carbide developed a new type of molecular sieve now known as silicalite (6). Silicalite is composed of pure silicon dioxide. It is resistant to corrosive agents except for hydrofluoric acid and strong alkalis and is stable to temperatures in excess of 1000°C (7).

Initial studies performed at the Ames Laboratory proved that sulfur dioxide was selectively and quantitatively adsorbed from stack gases and synthetic stack

gases on silicalite (7, 8). The effectiveness combined with the stability of silicalite suggested utility for combustion gas desulfurization.

The objectives of the present work at the Ames Laboratory are aimed towards hot gas cleanup. Studies being performed include the following areas:

- Evaluating the adsorption properties;
- Determining if trace gases are adsorbed;
- Elucidating conditions under which adsorbed sulfur dioxide is converted, in-situ, to sulfur trioxide;
- Determining efficient conditions for regeneration of silicalite and recovery of SO_2 ;
- Evaluating the economic feasibility of the overall process.

EXPERIMENTAL

Adsorbent and Gases - A granular molecular sieve, designated as S-115, was obtained from Union Carbide Corporation and used in all studies. Pure gases and synthetic stack gases were obtained from Matheson.

Adsorption Studies - The apparatus used in adsorption experiments is depicted in Figure 1. A synthetic stack gas at high pressure is mixed with nitrogen to obtain the desired SO_2 concentration. The gas is preheated to the desired temperature and passed through an adsorption bed. At temperatures below 650°C , the adsorbent is retained in stainless steel tubing and adsorption pressures are controlled by a regulator at the bed end. At temperatures greater than 650°C , the adsorbent is retained in quartz tubing and only low pressures (1 atmosphere) are used. Effluents from the bed pass through a 10-cm flow cell in a u.v. spectrophotometer (Varian, Cary D-219), and SO_2 concentrations are continuously monitored based upon absorbance at 284 nm.

Breakthrough Curves - Adsorption studies result in breakthrough curves as depicted in Figure 2. Interpretation of these plots of SO_2 concentrations in effluent gases vs. volume of gas passing through an adsorption bed is performed using established techniques (9, 10). Data obtained are: capacity - the amount of sulfur dioxide accumulated per gram of silicalite; adsorption rate; and minimum bed depth - the bed depth required for efficient adsorption.

Adsorption Capacity - Adsorption capacity determined from breakthrough curves is confirmed by determining the total sulfur content of spent silicalite using a total sulfur analyzer (Fisher).

Desorption of Sulfur Dioxide - Conditions for desorption of sulfur dioxide were determined by thermogravimetric analysis (TGA) of spent silicalite. An aliquot of spent silicalite was placed in a thermal analysis unit (DuPont) and weight was measured vs. temperature under a controlled atmosphere. In addition, studies were performed using a total sulfur analyzer in which sulfur dioxide evolution was determined at discrete temperatures.

RESULTS AND DISCUSSION

Adsorption Parameters. The capacity of silicalite as a function of adsorption temperature is given in Figure 3. As can be seen, below $\sim 350^\circ\text{C}$, the amount of sulfur dioxide accumulated decreases as temperature increases. This is expected. Above 350°C , however, there is an increase in capacity. This indicates a change in adsorbent structure or a different adsorption mechanism, perhaps chemisorption. X-ray diffraction analysis and Fourier Transform Infrared

Spectroscopic studies of spent silicalite reveal no evidence of chemisorption or of structural changes. Thus, the mechanism for adsorption at high temperature has not yet been determined. Even in the absence of a mechanism for high-temperature adsorption, the fact that sulfur dioxide is accumulated at temperatures in excess of 500°C make silicalite uniquely suited for cleanup of hot gases.

For hot gas cleanup, adsorption must also be effective at high pressures. As shown in Figure 4, at 500°C, the capacity of silicalite actually increases by a factor of about two when pressure is increased from one to ten atmospheres. Previous studies indicated that sulfur dioxide is adsorbed on silicalite as a liquid (8). The beneficial effects of pressure are consistent with liquefaction.

As shown in Figure 5, capacity increases as SO₂ concentration increases. With pure sulfur dioxide, the capacity is limited only by the pore volume of the adsorbent. The increase in capacity with increasing SO₂ concentration is of great practical significance for the desulfurization of combustion gases. Combustion of high-sulfur coals, which would lead to higher sulfur dioxide concentrations in gases, would not require proportionally larger desulfurization units.

The rate of adsorption has been found to vary from 6×10^{-4} cm³/gm-m to 22×10^{-4} cm³/gm-m over the conditions studied. High adsorption rates are typical of molecular sieves. Critical bed depth requirements have been found to vary from <1 to 4 cm. This is a consequence of the high adsorption rates. Back pressures created by a 3-m bed depth will be 0.1 psi. This is low, but even lower back pressures could be obtained readily because the required bed depth is less than 0.04 m. Back pressure is of great importance because of the cost of moving massive volumes of gas created in combustion against even small back pressures.

Adsorption of Trace Constituents - Work on the adsorption of trace constituents of combustion gases on silicalite is in progress. This work is of importance because irreversible adsorption of even a trace constituent of a combustion gas on silicalite would lead to a long-term decrease in capacity available for sulfur dioxide accumulation. No gases studied previously are retained as well as is sulfur dioxide. Thus, no problems are anticipated.

In-Situ Conversion of SO₂ to SO₃ - Previous work (8) has shown that sulfur dioxide can be converted to sulfur trioxide during adsorption or desorption on silicalite. Conditions for conversion were not defined. In the present work, conversion has been observed only at temperatures in excess of 650°C with stainless steel containers or in excess of 800°C with quartz containers. Detailed studies have not yet commenced.

Regeneration of Silicalite and Recovery of Sulfur Dioxide - Initial studies on the regeneration of silicalite indicate that thermal desorption in an oxidizing atmosphere results in recovery of capacity. As shown in Figure 6, TGA studies show that the temperature required for desorption of sulfur dioxide is determined by the temperature at which it was adsorbed. This phenomena has not yet been explained.

Preliminary Economic Evaluation - Silicalite is usable for removing sulfur dioxide from hot combustion gases and no other viable process exists, thus silicalite adsorption is the most economical process available. Sufficient data are not yet available for rigorous cost evaluations, but comparisons can be made with wet-lime processes used for flue gas desulfurization. Capital costs for

silicalite adsorption are likely to be much lower than for lime processing. The back pressure of silicalite is less than one-tenth that from lime scrubbers which eliminates the need for blowers. The gas is desulfurized without cooling which eliminates the need for reheaters.

Energy costs for silicalite adsorption will be comparable or less than those for lime scrubbers. Energy required for blowers and gas reheating is eliminated, but energy is needed for desorption of sulfur dioxide. For a worst-case scenario (regeneration at 400°C above adsorption temperature, no heat recovery, low-sulfur coal) approximately 640,000 BTU would be required to regenerate silicalite used to remove SO₂ from gases produced by one ton of coal. This would amount to less than 3% of the energy input.

Slurry disposal costs associated with wet-lime scrubbing are eliminated with silicalite adsorption and modest credits for sulfur dioxide sales are accrued. Because disposal costs are highly site specific and sulfur dioxide prices are volatile, the magnitude of the advantage for silicalite adsorption cannot be evaluated for general cases.

Adsorbent costs for silicalite adsorption or sulfur dioxide are likely to be higher than for lime scrubbing. The costs associated with lime scrubbing include the cost of lime, the availability of limes, and indirectly the costs associated with lime disposal. With silicalite, the predominant cost will be adsorbent attrition. Previous studies with silicalite indicate attrition rates of far less than 0.5% per adsorption/regeneration cycle are obtainable (11). In the present work, attrition rates have not yet been determined. If attrition is less than 0.1% per cycle, adsorbent costs will be comparable with the cost of lime. Determining low attrition rates requires repeated, time-consuming work that is in progress.

CONCLUSIONS

Adsorption of sulfur dioxide on silicalite molecular sieve provides an effective means for removing sulfur dioxide from hot combustion gases. Preliminary data indicate the process will be economically viable. Continued studies to define regeneration conditions precisely and to determine adsorbent attrition rates are in progress.

ACKNOWLEDGEMENTS

Ames Laboratory is operated for the U. S. Department of Energy by Iowa State University under Contract W-7405-ENG-82. This work was supported by the Assistant Secretary for Fossil Energy, Office of Direct Coal Utilization, through the Morgantown Energy Technology Center.

The authors greatly appreciate the support and advice provided by Richard Markuszewski, and the assistance of James Pollard with total sulfur determinations, of Surender Kaushik with TGA determinations, of Glenn Norton with XRD determinations, and of Navid Shah with economic evaluations.

REFERENCES

- (1) W. E. Moore, "Proceedings of the 5th Annual Contractors Meeting on Contaminant Control in Coal-Derived Gas Streams," U. S. Department of Energy, Morgantown, West Virginia, May 1985, p. 1.

- (2) C. J. Drummond and D. F. Gyorke, "Fossil Fuels Utilization - Environmental Concerns," ACS Symposium Series 319, Washington, D.C., p. 146 (1986).
- (3) D. A. Martin and F. E. Brantley, "Selective Adsorption and Recovery of Sulfur Dioxide from Industrial Bases by Using Synthetic Zeolites," U. S. Bureau of Mines Report 6321 (1973).
- (4) D. Bienstock, J. H. Field, and J. G. Myers, "Process Development in Removing Sulfur Dioxide from Hot Flue Gas," U. S. Bureau of Mines Report 5735 (1960).
- (5) J. J. Collins, L. L. Fornoff, K. D. Manchanda, W. C. Miller and D. C. Lovell, Chem. Eng. Pro. 70(6) 84 (1974).
- (6) E. M. Flanigan, J. M. Bennett, R. W. Grose, J. P. Cohen, R. L. Patton, R. M. Kirchner, and J. V. Smith, Nature 271(9) 512 (1978).
- (7) G. M. W. Shultz-Sibbel, C. D. Chriswell, D. T. Gjerde, J. S. Fritz and W. E. Coleman, Talanta 29 447 (1982).
- (8) C. D. Chriswell and D. T. Gjerde Anal. Chem. 54 1911 (1982).
- (9) G. S. Bohart and E. Q. Adams J.A.C.S. 42 523 (1920).
- (10) R. S. Ramalho, "Introduction to Wastewater Treatment Processes," Academic Press, New York, 1983.
- (11) C. D. Chriswell and H. R. Burkholder, unpublished data, 1981.

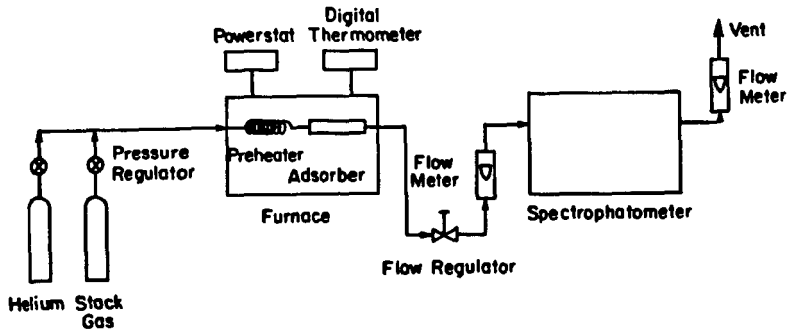


Figure 1. Schematic of apparatus used for SO₂ adsorption from hot, high-pressure gases.

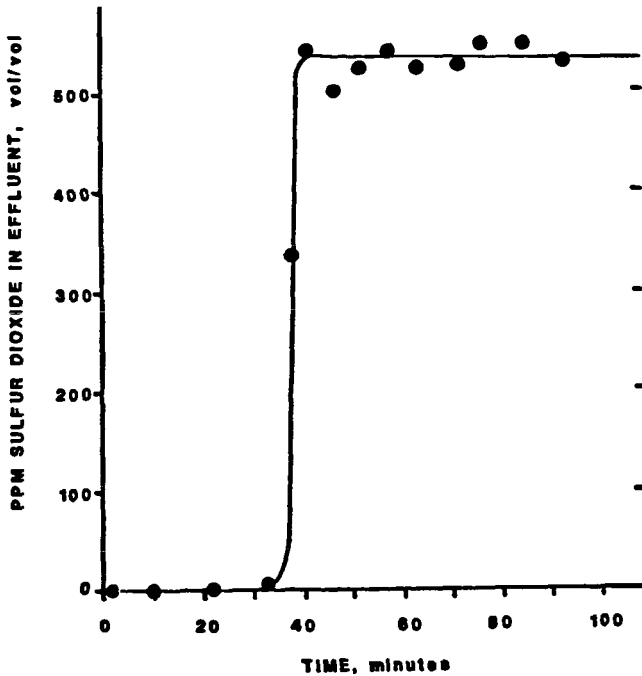


Figure 2. Typical breakthrough curve resulting from SO₂ adsorption on silicalite molecular sieve.

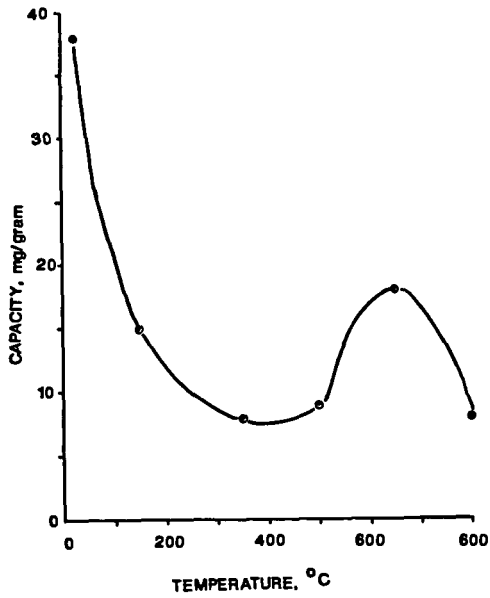


Figure 3. Adsorption capacity of silicalite for SO_2 as a function of adsorption temperature.

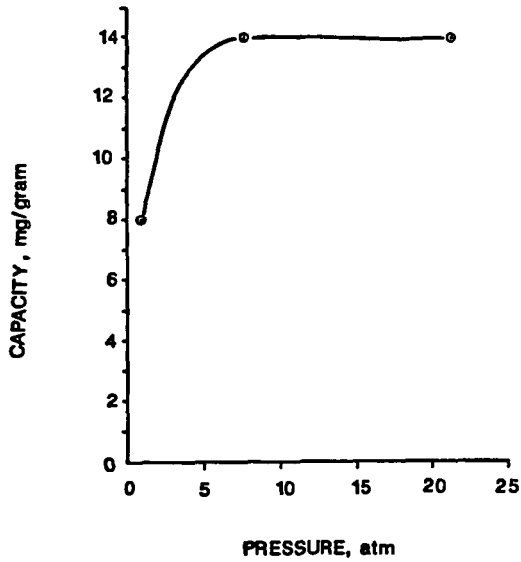


Figure 4. Adsorption capacity of silicalite for SO_2 as a function of adsorption pressure.

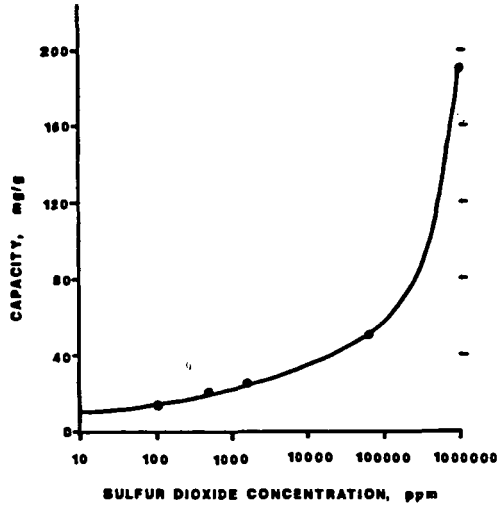


Figure 5. Adsorption capacity of silicalite for SO_2 as a function of SO_2 concentration in influent gas.

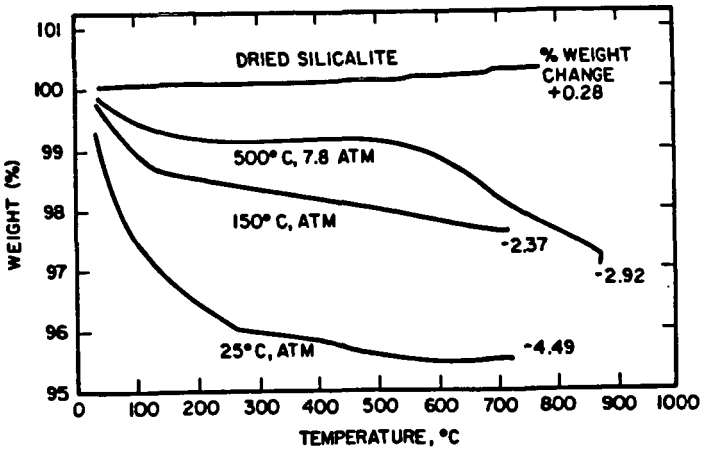


Figure 6. Thermogravimetric analysis and silicalite adsorbents containing SO_2 adsorbed under identified conditions.

REACTIONS INVOLVING HYDROPEROXIDE FORMATION IN JET FUELS

By

John M. Watkins, Jr.*, George W. Mushrush and Robert N. Hazlett
*GEO-Centers, Inc., Suitland, MD 20746
The Naval Research Laboratory, Code 6180
Washington, D.C. 20375-5000.

INTRODUCTION

Hydroperoxides in jet fuels attack elastomers in aircraft fuel systems with consequent leaks or inoperation of fuel controls. Problems have been associated with Jet A, JP-4, and JP-5 jet fuels. The first reported incidents occurred with Jet A in Japan in 1962 when fuel hoses of neoprene or nitrile rubber cracked and leaked (1). In 1976 the U.S. Navy experienced attack on neoprene fuel pump diaphragms on jets operating in the Philippines (2). More recent problems have been encountered in Thailand with JP-4 when Buna-N O-rings cracked and leaks from fuel pumps occurred. All incidents involved fuels which had been hydrotreated and had peroxide levels from 1 to 8 milliequivalents of active oxygen per kilogram of fuel (peroxide number, P.N.).

Examination of fuels refined by different processes has indicated that significantly higher peroxide concentrations exist in fuels which have been severely hydrotreated. The U.S. Navy has continuing concerns with this topic due to increasing hydrogenation for jet fuel processing. In addition, shale-derived fuel production will involve more extensive and higher pressure hydrotreatment. It has been demonstrated that sulfur compounds in lubricating oils act as antioxidants by decomposing peroxides (3). It is believed that hydrogenation is responsible for removing natural inhibitors, including sulfur compounds, to peroxide formation.

Hydroperoxide concentration has been found to be a factor in fuel instability. Fuel degradation is observed to occur under long-term low-temperature storage conditions (storage stability) as well as short-term high-temperature stress (thermal oxidative stability) (4-7). The latter situation is found during flight conditions, where fuel serves as a coolant on its path to the combustion chamber. Although slight thermal degradation is found to occur in nonoxidizing atmospheres, the presence of oxygen or active species such as hydroperoxides will greatly accelerate oxidative degradation

as well as significantly lower the temperature at which undesirable changes in fuel take place. The rates of reactions in autoxidation schemes are dependant on hydrocarbon structure, heteroatom concentration, oxygen concentration, and temperature (8-10). If sufficient oxygen is present, the hydroperoxides will reach a high level. If the available oxygen is low, but the temperature raised, the hydroperoxide concentration will be limited by free radical decomposition. Under these conditions, fuel degradation can be associated with both hydroperoxide formation and decomposition.

Several solutions to the problem of fuel peroxidation have been suggested. Antioxidants have been mandated by some authorities, particularly for hydrotreated fuels. Viton elastomers and other materials have been proposed as replacement materials but their low temperature properties make them marginal for aircraft use. Clay filtration has been suggested as a means for field removal of hydroperoxides but this treatment has been found to be too expensive (2). Although hindered phenols have given satisfactory peroxide control, those phenols which are permitted in the jet fuel specifications were developed for gum control in gasoline. Their effectiveness for peroxide control was found to be marginal, depending on structure (11). It is necessary to investigate the relationship of temperature on peroxide concentration in fuel as it relates to peroxide formation as well as fuel stability.

Sulfur is the most abundant heteroatom present in jet fuels (up to 0.4% allowed by specifications). Deposits formed in jet fuel in the presence of oxygen contain a higher percentage of sulfur than that present in the fuel itself (12). The formation of these deposits has been attributed to the participation of sulfides, disulfides, and thiols (mercaptans) (13). In jet fuels that have been deoxygenated, sulfides and disulfides have been found to lead to increased solid formation (14). Examination of the reactions between both alkyl and aromatic thiols with tert-butylperoxide have indicated that aromatic thiols are more reactive than other classes of sulfur compounds with hydroperoxides. The reaction of thiophenol with tBHP was found to produce trace amounts of sulfonic acid while depleting the amount of both reactants in solution (15). It is desirable to test the relationship between sulfur compound reactivity and peroxide formation using an aryl thiol as a model dopant under accelerated storage conditions.

This paper reports on the hydroperoxide formation in hydrotreated JP-5 jet fuels at various temperatures, in both the presence and absence of antioxidants. The results of using thiophenol as a model dopant for four stable, hydrotreated jet fuels under 65C accelerated storage conditions and the effect on peroxide formation versus added sulfur concentration are also reported.

EXPERIMENTAL

Fuels and Reagents. The fuels examined for the temperature effects study included a shale JP-5 with antioxidant, a hydrotreated petroleum JP-5 with and without antioxidant, and a petroleum JP-4 without antioxidant. The four fuels investigated for the sulfur versus peroxide concentration study were the same Shale-II JP-5 used in the temperature study (J-22), a Jet-A, a Hydrocracked JP-5 and a Hydrofined JP-5 from Esso Petroleum Corporation, Ontario, Canada. Thiophenol was obtained from Aldrich Chemical Co. and was

distilled in vacuo to 99.9% purity.

Method. Tests were carried out in brown borosilicate glass bottles, 500 ml total capacity, capped with teflon liners, containing 300 ml of fuel per bottle. Test for temperature effects on peroxidation were carried out at 43, 65, 80 and 100C. To test the relationship of added sulfur to peroxide concentration, duplicate samples of the four other fuels were prepared, with 0.10 and 0.05% sulfur in the form of thiophenol weighed into one sample of each fuel. Stress tests were conducted at 65C for five weeks. Samples were analyzed weekly for peroxide concentration by ASTM method D3703-85. Sulfur concentration was monitored weekly with a Tracor 565 gas chromatograph equipped with a sulfur specific 700A Hall electrolytic conductivity detector.

RESULTS AND DISCUSSION

Rolls-Royce defined the peroxidation potential of a fuel with an accelerated 100C test for 24 hours (1). The relevance of this test to ambient storage conditions was of interest, so stress tests were conducted at 43, 65, 80 and 100C.

The peroxide numbers for the different temperatures are listed in Table I. The stress times were selected according to the Arrhenius relation, namely doubling (or halving) of reaction rate for every 10°C change in temperature, and then modified based on previous results from our laboratory. Thus time factors of 30:1 and 10:1 were used for 43C and 65C test instead of the calculated values of 52:1 and 11.3:1. Columns in the Table are labeled "equivalent hours at 100C." The actual storage times at the several temperatures are shown at the end of the data table.

Data for the two JP-5 samples, with and without oxidant are plotted in Figures 1 and 2. Time factors for multiplying the abscissa are listed on the graphs for the various temperatures.

The data reveal appreciable variation in peroxide number as a function of time, temperature and fuel. Two fuels, petroleum JP-5 and JP-4 both without antioxidant, show fair agreement between the temperatures based on equivalent time periods. In at least two cases (Fuels 3 and 4), peroxide levels at all times were lower at the lower temperatures. With the two fuels containing antioxidants (Fuels 1 and 3), results at the lower temperatures were quite different from results at the higher temperatures, and therefore not predictable from the higher temperature test.

Important difference in fuel response to temperature is illustrated by comparing Figures 1 and 2. The hydrotreated JP-5 without antioxidant (Fuel 2), Figure 1, produces peroxide at a linear rate with respect to time for the initial portion of the tests. The time factors are also reliable in the 1-3 day equivalent time frame.

Shale-II JP-5 (Fuel 1) containing an antioxidant behaves quite differently. Peroxidation follows an exponential rate. The most probable explanation for this observation is the depletion with time of the antioxidant. The rate of peroxidation was not predictable from the time factors. Specifically, the rate was much faster at 80 and 100C than the low temperature data would indicate.

Based on these observations, the 65C stress test was chosen for the sulfur concentration study. Added sulfur concentrations of 0.10 and 0.05% sulfur (weight/volume) were used. The data for these tests are represented in

Tables II and III respectively.

For both sulfur concentrations, the control samples, fuel only, exhibited similar behavior. Differences in actual peroxide numbers between the two tests could be attributed to thermostatic differences in the ovens that were used. It was interesting that in Jet A peroxide formation occurred in a cyclic pattern. The petroleum derived JP-5 samples formed peroxides at a greater rate than the shale JP-5 or Jet A.

The most important aspect of both sets of data was that the samples doped with sulfur in the form of thiophenol did not undergo peroxidation as rapidly as the fuel by itself. In fact, thiophenol addition eliminated ROOH present in starting samples in most tests, and after the first week in the other tests. In the samples doped with 0.10% sulfur, peroxide formation was not observed until the fourth week of the stress test. When the concentration of added sulfur was reduced (halved) peroxide formation began one week earlier with three of the fuels, indicating a relationship between added sulfur concentration and peroxide formation (or peroxide inhibition). Neither of the doped samples of the hydrocracked JP-5 showed evidence of peroxide formation throughout the duration of the tests.

The sulfur concentration of the samples was found to decrease throughout the tests as measured by the sulfur specific detector on the gas chromatograph. The emergence of new peaks on the chromatogram indicated the formation of new sulfur-containing compounds, however concentrations were too low to permit identification. Since aromatic thiols are quite reactive in the presence of peroxides, the thiophenol most likely undergoes oxidation by the peroxide species. These reactions could be similar to other observed liquid phase oxidation reactions that take place between thiophenol and t-butyl hydroperoxide (15).

CONCLUSIONS

The effect of adding sulfur in the form of an aromatic thiol, thiophenol, was significant to peroxide formation. Thiophenol has been found to act as an inhibitor or controller of peroxide formation in Jet A, Shale-II derived JP-5, and petroleum derived JP-5. Hydrotreated jet fuels exhibited higher peroxide formation and concentration than other fuels. Hydrotreatment reduces the sulfur content of the fuel, which removes those naturally occurring sulfur compounds which act as inhibitors to peroxide formation. There appeared to be a "critical concentration" of sulfur at which peroxide formation was inhibited. If this concentration was decreased or consumed, peroxidation took place in an uncontrolled manner.

LITERATURE CITED

1. Smith, M., "Aviation Fuels," Chap. 51, G. T. Foulis & Co., Ltd., Henley-on-Thames, England, 1970.
2. Shertzer, R. H., "Aircraft Systems Fleet Support/Organic Peroxides in JP-5 Investigation," Final Report NAFPC -LR-78-20, Naval Air Propulsion Center, Trenton, N. J., Sep. 1978.
3. Dension, G., Ind. Eng. Chem., 36, 477, 1944.
4. Hazlett, R. N. "Free Radical Reactions Related to Fuel Research" in "Frontiers of Free Radical Chemistry" p. 195, ed. W. Pryor, Academic Press, New York, 1980.
5. Taylor, W. F., Ind. Eng. Chem. Prod. Res. Dev., 13, 133, 1974.
6. Scott, G., "Autoxidation," Chap. 3, Elsevier, Amsterdam, 1965.
7. Taylor, W. F. and Wallace, T. J., Ind. Eng. Chem. Prod. Res. Dev., 6, 258, 1967.
8. Morse, B. K., J. Am. Chem. Soc., 87, 3375, 1957.
9. Hiatt, R. R. and Irwin, K. C., J. Org. Chem., 33, 1436, 1968.
10. Denisov, E. T., "Liquid Phase Reaction Rate Constants," IFI/Plenum, New York, 1974.
11. Hazlett, R. N., Hall, J. M., Nowack, C. J., and Craig, L., "Hydroperoxide Formation in Jet Fuels," Conference Proceedings, Israel Institute of Petroleum and Energy, Conference on Long Term Storage Stabilities of Liquid Fuels, 1983.
12. Wallace, T. J., "Adv. Petroleum Chem. and Refining," Chap. 8, Wiley-Interscience, New York, 1964.
13. Taylor, W. F. and Wallace, T. J., Ind. Eng. Chem. Prod. Res. Dev., 7, 258, 1968.
14. Taylor, W. F., Ind. Eng. Chem. Prod. Res. Dev., 13, 133, 1974. *ibid* 15, 64, 1976.
15. Mushrush, G. W., Hazlett, R. N., Hardy, D. R., and Watkins, J. M., "Liquid Phase Oxidation of Sulfur Compounds," Conference Proceedings, 2nd International Conference on Long Term Storage Stabilities of Liquid Fuels, in press, 1986.

TABLE I

Peroxidation at Various Temperatures

Fuel	Temp. °C	Time Factor	Equivalent Hours at 100°C							
			3	7	24	48	72	96	168	
1. Shale JP-5 w/A.O.	43	30:1	-	-	1.03	1.10	1.38	1.74	2.66	
	65	10:1	-	-	1.45	1.80	2.44	3.90	8.69	
	80	4:1	-	1.10	2.53	7.43	18.4	43.3	1.48	
	100	1:1	.85	1.05	2.66	9.11	23.3	19.3	0.96	
2. Petroleum JP-5 No A.O.	43	30:1	-	-	13.2	41.0	82.5	111	133	
	65	10:1	-	-	13.5	53.3	86.3	121	198	
	80	4:1	-	7.41	34.3	60.7	82.4	95.2	78.9	
	100	1:1	1.61	5.52	24.6	48.0	66.8	72.0	61.5	
3. Petroleum JP-5 w/A.O.	43	30:1	-	-	0	0	0	0	0	
	65	10:1	-	-	0	0	0	0	.12	
	80	4:1	-	0	0	.10	.16	.35	39.7	
	100	1:1	0	0	0	.29	.78	2.31	42.9	
4. Petroleum JP-4 No A.O.	43	30:1	-	-	.07	.03	.12	.14	.19	
	65	10:1	-	-	.10	.16	.12	.16	.14	
	80	4:1	-	0	.24	.25	.25	.20	.30	
	100	1:1	.07	.10	.22	.23	.22	.26	.22	
All Fuels	43	ACTUAL STORAGE TIMES					60d	90d	120d	210d
	65	3.8d	8.8	30d	30d	20d	30d	30d	40d	70d
	80	30h	70h	10d	10d	8d	12d	16d	28d	
		12h	28h	4d	4d	8d	72h	96h	168h	
	100	3h	7h	24h	48h					

TABLE II
 Jet Fuel Peroxidation at 65°C with Added Thiophenol
 0.10% Sulfur Dopant

Week	<u>Shale-II JP-5</u>		<u>Jet A</u>		<u>Hydrocracked JP-5</u>		<u>Hydrofined JP-5</u>	
	Control	Doped	Control	Doped	Control	Doped	Control	Doped
0	0.25	0.25	0.00	0.00	0.00	0.00	0.16	0.16
1	0.24	0.00	0.19	0.00	0.18	0.00	0.57	0.00
2	0.31	0.00	0.44	0.00	0.49	0.00	1.16	0.00
3	0.37	0.00	0.19	0.00	1.10	0.00	1.73	0.00
4	0.51	1.29	0.40	0.51	4.08	0.00	5.38	0.26
5	0.48	0.97	0.26	0.40	10.82	0.00	8.47	0.25

TABLE III
 Jet Fuel Peroxidation at 65°C with Added Thiophenol
 0.05% Sulfur Dopant

Week	<u>Shale-II JP-5</u>		<u>Jet A</u>		<u>Hydrocracked JP-5</u>		<u>Hydrofined JP-5</u>	
	Control	Doped	Control	Doped	Control	Doped	Control	Doped
0	0.69	0.00	0.12	0.00	0.10	0.00	0.24	0.00
1	0.70	0.00	0.18	0.00	0.60	0.00	1.58	0.00
2	0.73	0.00	0.16	0.00	2.09	0.00	6.01	0.00
3	0.94	0.45	0.28	0.54	12.41	0.00	37.66	0.61
4	1.11	0.68	0.26	0.22	25.27	0.00	62.05	0.51
5	1.56	0.88	0.29	0.81	56.67	0.00	59.92	0.25

FIGURE 1

HYDROPEROXIDE FORMATION
AT VARIOUS TEMPERATURES
--HYDROTREATED JP-5--NO A.O.

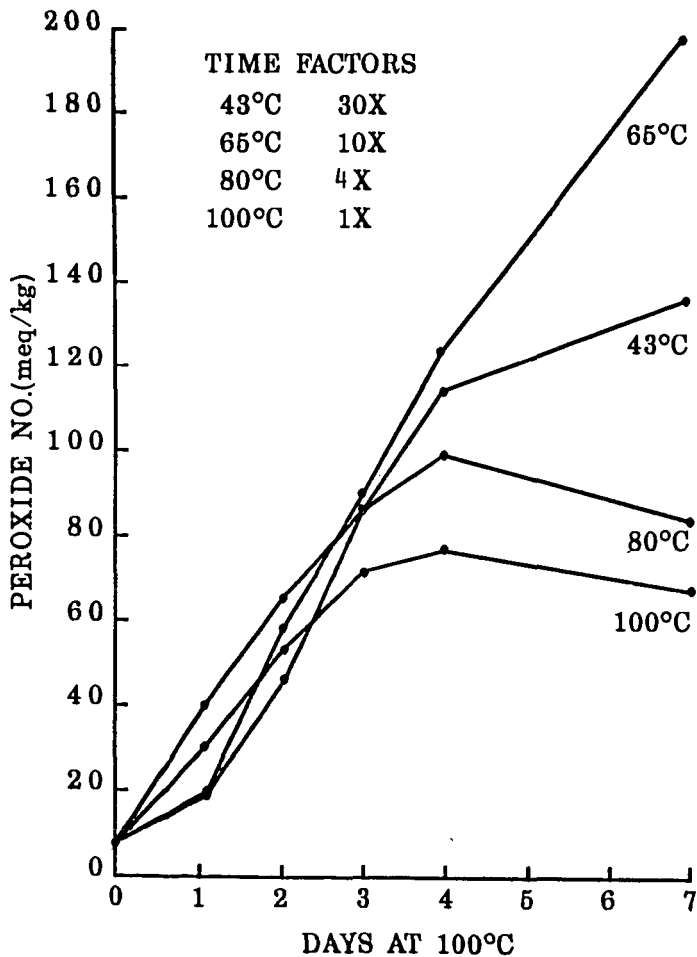
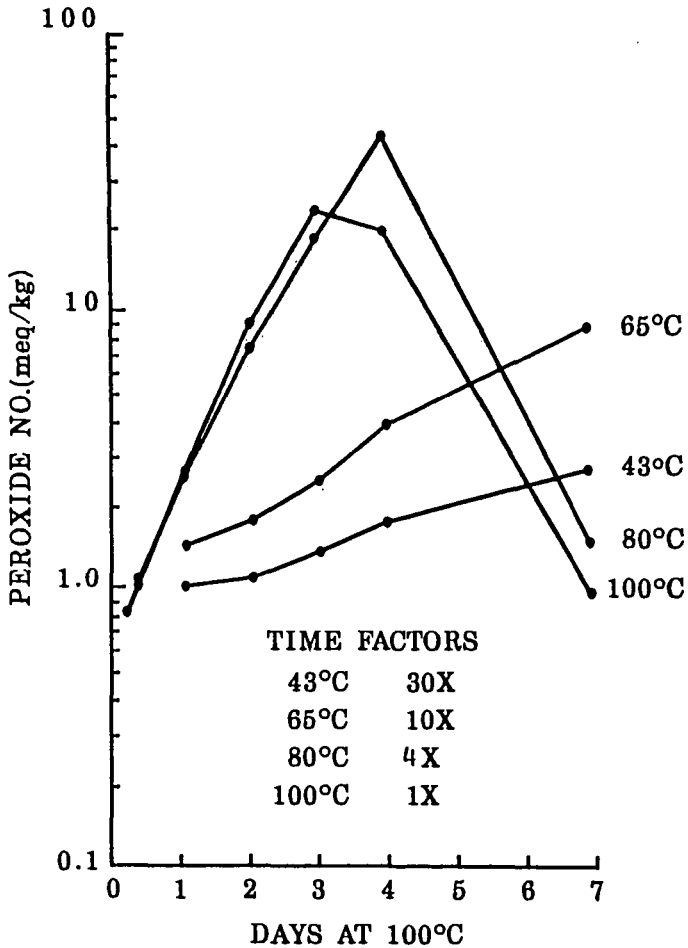


FIGURE 2

HYDROPEROXIDE FORMATION
AT VARIOUS TEMPERATURES
--SHALE-II JP-5--WITH A.O.



LIQUID PHASE OXIDATION OF THIOPHENOL AND OLEFINS
BY OXYGEN AND t-BUTYL HYDROPEROXIDE

By

George W. Mushrush, John M. Watkins^a, Robert N. Hazlett,
Dennis R. Hardy and Harold G. Eaton
The Naval Research Laboratory Code 6180
Washington, D.C. 20375-5000 and
^aGEO-CENTERS, Inc. Suitland, MD 20746

INTRODUCTION

In supersonic Navy aircraft, aerodynamic heating can cause metal skin temperature to rise to high levels. At mach 2.7, it has been estimated that the fuel in an uninsulated wing tank could reach 430F (1). Hydrocarbon fuels subjected to such temperatures have been shown to undergo considerable degradation. This observed degradation can be manifested by the formation of deposits on filters, in nozzles and on combustor surfaces (2-5). These deposits are the consequence of free radical autoxidation reactions. Trace levels of sulfur compounds have been found to influence the deposit formation process. It has been shown that jet fuels low in sulfur content are relatively stable and that fuels of high sulfur content are fairly unstable (6,7). Presently, it is not possible to relate the observed instability to specific sulfur species. Heteroatoms (oxygen, nitrogen and sulfur) and ash have been found to comprise 40 percent of such deposits (8). The sulfur content of these deposits has been found to vary from 1 to 9% (9). Sulfur (0.4%) is the most abundant heteroatom present in the fuel itself.

Deposits formed in jet fuel in the presence of oxygen contained a greater percentage of sulfur than that present in the fuel itself (10). In previous work in our laboratory, it was observed that thiols, sulfides and aldehydes could be readily oxidized by hydroperoxides (11-13).

The rates of the reactions in autoxidation schemes are dependent on structure, oxygen concentration and temperature (14-16). Catalysts, free radical initiators and inhibitors can materially alter both the rate and the oxidation pathways (17,18).

Although slight thermal deterioration of fuel is known to occur in non-oxidizing atmospheres, the presence of elemental oxygen will greatly

accelerate the deterioration of fuel properties as well as significantly lower the temperature at which undesirable products are formed. Thus the stability of jet fuels is frequently dependent upon the nature of potential autoxidation pathways which can take place under aircraft operating conditions.

If sufficient oxygen is present, the hydroperoxide concentration will reach a high level. If the available oxygen is low, but the temperature is raised, the hydroperoxide level will be limited by free radical decomposition. This regimen, low oxygen and increasing temperature, is similar to the environment in an aircraft fuel system. In this situation fuel degradation can be associated with the reaction of hydroperoxides with the other moieties in the fuel.

This paper is concerned with the reaction between a primary autoxidation product, a hydroperoxide, with thiophenol in the presence of the active olefins indene and styrene. The reactions were carried out in deaerated benzene with *t*-butyl hydroperoxide or in benzene with an oxygen overpressure.

EXPERIMENTAL

Reagents. *tert*-Butyl hydroperoxide, tBHP, (90%), thiophenol, indene and styrene were obtained from Aldrich Chemical Co. They were distilled in vacuo to 99.9% purity. Benzene (Aldrich Gold Label) was refluxed and distilled from calcium hydride.

Method. The reactions were carried out in sealed borosilicate glass tubes. The reagents (typically $3\text{-}9 \times 10^{-4}$ mol of tBHP and 6×10^{-4} mol of both thiophenol and olefin in 0.6ml of solvent) were weighed into 6 in. long, 1/4-in. o.d. borosilicate glass tubes closed at one end and fitted at the other with a stainless steel valve via a Swagelok (teflon ferrules) fitting. The tube was attached to a vacuum system, cooled to 77K and subjected to several freeze-pump-thaw cycles. For those runs in oxygen, the solution was bubbled extensively with oxygen, a 40 - 45 psi over pressure of oxygen was then added. The tube was then subsequently flame-sealed below the valve. The ullage volume (0.30 ml) was kept constant for all runs. The deaerated samples were warmed to room temperature and immersed in a Cole-Parmer fluidized sand bath. The temperature was controlled by a Leeds and Northrup Electromax III temperature controller. The total pressure during each run was estimated to be 5.1 atm for the runs in benzene solvent. After the reaction period (15, 30, 60 min) the sealed tube was quenched to 77K and opened.

The samples were analyzed by combined GC/MS (EI mode). The GC/MS unit consisted of a Hewlett-Packard Model 5710 GC, a H-P Model 5982A mass spectrometer, and a Ribermag SADR GC/MS data system. An all glass GC inlet system was used in conjunction with a 0.31 mm x 50 m SP-2100 fused silica capillary column.

Gases formed during the reaction were analyzed using a Perkin-Elmer Model Sigma 2 gas chromatograph equipped with a 6 ft. 5A Molecular Sieve column. In this mode, the column was operated at 55C. The chromatogram was recorded and integrated on a Hewlett-Packard Model 3390A reporting integrator. An external standard was used for calibration. A gauge measured the pressure in the sample loop at the time of analysis.

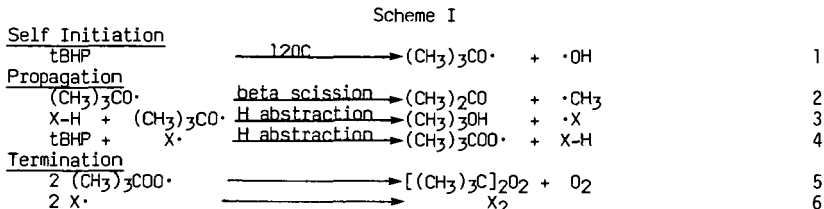
RESULTS AND DISCUSSION

At temperatures of 120C or greater, tBHP decomposes rapidly by an autoinitiated pathway (19,20). The major reaction pathway in the 120C decomposition of tBHP involves attack by free radicals present in the solution. The detailed mechanism is complicated since free radicals are sensitive to structural, solvent and stereoelectronic effects.

The results in Tables 1 and 2 illustrate the product distribution for the tBHP, styrene, indene and thiophenol derived products. The quantities in the tables are expressed in terms of mole percent conversion from the moles of reactant originally present. Products derived solely from tBHP (for example acetone) are calculated based on the starting amount of tBHP. The same is true for products from the thiophenol (i.e., phenyl disulfide). Oxidation products are calculated based on the moles of olefin originally present.

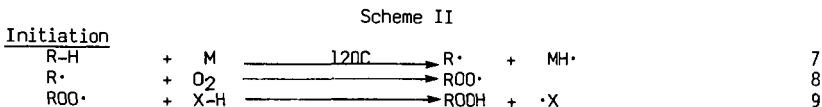
From tBHP, the major product was t-butanol. Small amounts of acetone, methane, isobutylene and the tBHP radical termination product, di-t-butyl peroxide, were also observed.

tBHP products The mechanism of autoinitiated tBHP decomposition can be depicted in Scheme I.



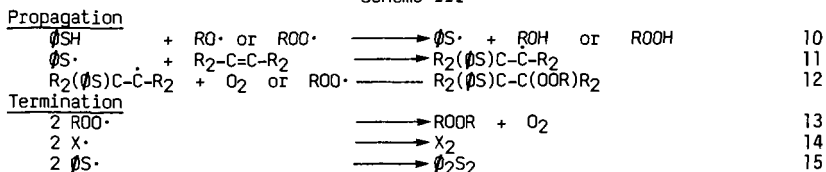
The greater yield of t-butanol compared to acetone, Tables 1 and 2, definitively show that hydrogen abstraction was favored over scission under the conditions of this study. Solvent participation was noted by the formation of trace quantities of toluene and other substituted benzenes from benzene.

The reaction mechanism, initiation step, in the presence of molecular oxygen can be depicted by Scheme II.



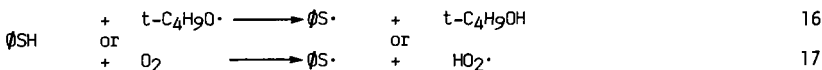
The reaction of the hydroperoxide, step 9, would then follow the same pathways as indicated for steps 1-6 in Scheme I. The reaction of thiophenol and active olefins with oxygen provides a useful co-variant of thiol chemistry termed "co-oxidation" (21). The radicals that result from either Schemes I or II could subsequently react with either the thiophenol and/or olefins that are present in the reaction mixture. This process can be described by Scheme III.

Scheme III

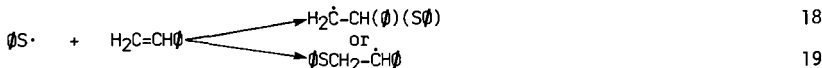


Styrene - thiophenol reaction products The major product, Table 1, observed was the addition product 1-phenyl-2-phenylthiyl ethane. Its yield at 15 min was 41.3% increasing to 71.2% at 30 min and decreasing to 68.3% at 60 min. Other products included: the 1-phenyl-1-phenylthiyl ethane isomer, 0.5% at 15 min increasing to 3.5% at 60 min; the dimer of styrene, 1,4-diphenyl butane, 0.2% at 60 min; 1-phenyl-2-phenylethyl sulfoxide, 1.7% at 15 min increasing to 5.8% at 60 min; 1-phenyl-2-phenylthiyl butane, 1.1% at 15 min decreasing to 0.9% at 60 min and phenyl thiosulfonate, 0.3% at 60 min. Trace products (< 0.1% yield) included: phenyl disulfide, 1-phenyl-2-phenylethyl sulfone, styrene oxide, phenyl methyl sulfide and 2-ethyl toluene. The product slate was the same for both oxygen and tBHP, but the yields of individual components varied significantly. In general, the tBHP reaction was faster as would be expected, than the reaction starting with elemental oxygen. In the presence of tBHP, the major product, 1-phenyl-2-phenylthiyl ethane, increased to 62.4% at 15 min and the sulfoxide product was more than doubled at 3.9% for the same time period.

The reaction of molecular oxygen or tBHP with thiophenol can proceed by the following chain mechanism (steps 16-17). The t-butoxy radical is more reactive than the t-butyl peroxy radical and consequently is a more probable reactant in such a mechanism (11).



The thiyl radical once formed can then react by several different pathways. In a solution with a high molar concentration of an active olefin, the reaction would proceed as shown in steps 18-19.



Equation 19 was the preferred pathway since it resulted in the more thermodynamically stable radical. The major product, 1-phenyl-2-phenyl thiyl ethane, then results by hydrogen abstraction. The other radical generated, equation 18, leads to one of the observed minor products, 1-phenyl-1-phenyl thiyl ethane. Other pathways could involve the reaction of radicals generated in steps 11 or 12 with additional olefin to give products of high molecular weight.

The sulfoxide product, phenyl-2-phenylethyl sulfoxide, could result from

several mechanisms. The most likely mechanism however, would be the reaction of the hydroperoxide with the sulfide formed in step 19. Expansion of the sulfur valence shell is probable in the processes involved in this step. The resulting sulfoxide once formed is quite stable, as can be seen from the gradual increase in yield, Table 1, at extended reaction time.

Table 1

Mole % Conversion for the Reaction of Styrene with Thiophenol and Oxygen or t-Butyl Hydroperoxide at 120°C

	CONVERSION (MOLE%)			
	Reaction Time (Min)			tBHP
	Oxygen			
	15	30	60	15
<u>Addition Products^a</u>				
1-phenyl-2-phenylthiyl ethane	41.3	71.2	68.3	62.4
1-phenyl-1-phenylthiyl ethane	0.5	1.5	3.5	1.4
phenyl-2-phenylethyl sulfoxide	1.7	4.9	5.8	3.9
phenyl disulfide	1.1	1.7	2.3	1.7
1,4-diphenyl-2-phenylthiyl butane	1.1	0.9	0.9	1.9
phenyl thiosulfonate	---	0.2	0.3	1.1
1,4-diphenyl butane	---	---	0.2	0.2
<u>Unreacted</u>				
styrene	34.7	2.0	1.6	13.2
thiophenol	33.2	7.1	5.8	25.2
<u>tBHP Products</u>				
acetone	---	---	---	0.9
t-butanol	---	---	---	57.1
di-t-butyl peroxide	---	---	---	0.1
isobutylene	---	---	---	2.3
<u>Trace Products^b</u>				
	2.2	4.3	6.6	3.2

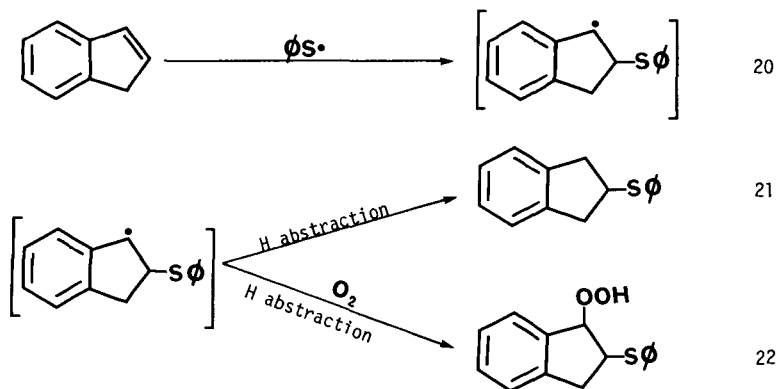
a. based on the starting moles of styrene

b. summation of small peaks

Indene - thiophenol reaction products The products from this co-oxidation reaction can be conveniently divided into primary and secondary reaction products. As shown in Table 2, the major primary reaction product was 2-phenylthiyl indan, 39.4 mole % at 15 min increasing to 58.2% at 30 min and then decreasing to 55.8% at 60 min. The secondary products were formed

by the spontaneous rearrangement of either 2-phenylthiyl-1-indanyl or 1-phenylthiyl-2-indanyl hydroperoxide. Neither hydroperoxide isomer was detected by GC/MS. The observed products from this rearrangement were: 2-phenylthiyl-1-indanol, 0.8% at 15 min increasing to 2.1% at 60 min; 2-phenylthiyl-1-indanone, 0.4% at 15 min increasing to 0.8% at 60 min; and 1-phenylthiyl-2-indanol, 0.2% at 15 min increasing to 0.4% at 60 min. Other products included: from the thiophenol, phenyl disulfide, 2.1% at 15 min increasing to 6.1% at 60 min and phenyl thiosulfonate, 0.1% at 15 min increasing to 0.5% at 60 min. From the 15 min run employing tBHP, products formed were: acetone, 0.7%; t-butanol, 54.3%; di-t-butyl peroxide, 0.5% and isobutylene, 3.2%. As shown in Table 2, many trace products (<0.1% yield) were formed. They were the result of oxidation of the indene, scission of the indene double bond or the more extensive oxidation of other products.

The processes for the reaction of oxygen or tBHP with thiophenol and indene proceeds as shown in Schemes I - III. The most probable step for the formation of the indanyl radical and its subsequent reactions are shown in steps 20-22. The thiyl radical can also undergo a dimerization reaction to produce the disulfide, step 15, and subsequently more extensive oxidation to yield the thiosulfonate product.



The 2-phenylthiyl indanyl radical, step 20, can react by several pathways. Hydrogen abstraction, step 21, would lead to the major observed product 2-phenylthiyl indan. Step 22, the reaction with oxygen would lead to the secondary product, 2-phenylthiyl-1-indanyl hydroperoxide. This secondary product was not detected by GC/MS, but the alcohols and ketones from its decomposition were found. Based on other hydroperoxide studies, it was not surprising that this hydroperoxide compound was not observed (11,12).

A comparison of the amounts of olefin and thiophenol remaining at different reaction times, Tables 1 and 2 indicates that the indene system is less reactive than styrene. The results at 15 min with tBHP also show that the indene system is less reactive. In the indene system, sulfoxides and

sulfones were only observed as minor products.

Table 2

Mole % Conversion for the Reaction of Indene with Thiophenol
and Oxygen or t-Butyl Hydroperoxide at 120C

CONVERSION (MOLE %)

	Reaction Time (Min)			tBHP
	Oxygen			
	15	30	60	
<u>Addition Products^a</u>				
2-phenylthiyl indan	39.4	58.2	55.8	48.3
2-phenylthiyl-1-indanol	0.8	1.7	2.1	1.6
1-phenylthiyl-2-indanol	0.2	0.4	0.4	0.4
2-phenylthiyl-1-indanone	0.4	0.8	0.8	0.6
phenyl disulfide	2.1	3.8	6.1	2.7
phenyl thiosulfonate	0.1	0.2	0.5	0.3
<u>Unreacted</u>				
indene	49.2	34.9	26.2	43.4
thiophenol	44.3	31.1	20.7	39.7
<u>tBHP Products</u>				
acetone	----	----	----	0.7
t-butanol	----	----	----	54.3
isobutylene	----	----	----	3.2
di-t-butyl peroxide	----	----	----	0.5
<u>Minor Products (0.1% or less)</u>				
1-indanone		2-indanone		
1-indanol		2-indanol		
toluene		1-methyl,2-ethyl benzene		
2-phenylsulphinyl-1-indanol				
1-phenylsulphinyl-2-indanol				
2-phenylsulphonyl-1-indanol				
1-phenylsulphonyl-2-indanol				
Trace Products ^b	3.2	3.1	4.6	2.9

a. based on the starting moles of indene.

b. summation of small peaks

CONCLUSION

There are similarities and differences in the styrene and indene systems. The major product in both systems was an addition product; Styrene and thiophenol in the presence of oxygen or tBHP at 120C formed 1-phenyl-2-phenylthiyl ethane while indene under the same conditions formed 2-phenylthiyl indan. The styrene system formed sulfoxides in appreciable yield while these compounds were not observed with the indene system. Indene formed alcohol and ketone products that were not observed with the styrene indicating a different mechanism for these products. Styrene was more reactive than the indene under the conditions of this study.

LITERATURE CITED

1. Chemical Week, 21, (Jan. 14, 1967).
2. Hazlett, R. N. and Hall J. M., "Chemistry of Engine Combustion Deposits"; Plenum Press: New York, 1985, page 245.
3. Taylor, W. F. and Wallace, T. J. Ind. Eng. Chem. Prod. Res. Dev. 6, 258 (1967).
4. Scott, G., "Atmospheric Oxidation and Antioxidants"; Elsevier: Amsterdam, 1965; Chapter 3.
5. Taylor, W. F., Ind. Eng. Chem. Prod. Res. Dev., 13, 133 (1974).
6. Taylor, W. F., Ind. Eng. Chem. Prod. Res. Dev., 15, 64 (1976).
7. Daniel, S. R. and Heneman, F. C., Fuel, 62, 1265 (1983).
8. Nixon, A. C., "Autoxidation and Antioxidants of Petroleum"; Wiley Interscience: New York, 1962.
9. Coordinating Research Council, "CRC Literature Survey on the Thermal Oxidation Stability of Jet Fuel"; CRC Report No. 509; CRC, Inc: Atlanta, GA, 1979.
10. Wallace, T. J., "Adv. Petroleum Chem. and Refining"; Wiley-Interscience: New York, 1964; Chapter 8.
11. Mushrush, G. W. and Hazlett, R. N., J. Org. Chem., 50, 2387 (1985).
12. Mushrush, G. W., Hazlett, R. N. and Eaton, H. G., Ind. Eng. Chem. Prod. Res. Dev., 24, 290 (1985).
13. Mushrush, G. W., Watkins, J. W., Hazlett, R. N. and Hardy, D. R., Ind. Eng. Chem. Prod. Res. Dev., In Review.
14. Morse, B. K., J. Am. Chem. Soc., 87, 3375 (1957).
15. Hiatt, R. R. and Irwin, K. C., J. Org. Chem., 33, 1436 (1968).
16. Denisov, E. T., "liquid Phase Reaction Rate Constants"; IFI/Plenum: New York, 1974.
17. Benson, S. W. and Shaw R., Organic Peroxides"; Wiley-Interscience: New York, 1970; Chapter 2.
18. Howard, J. A. and Ingold, K. U., Can. J. Chem., 47, 3797 (1969).
19. Mosher, H. S. and Durham, L. J., J. Am. Chem. Soc., 82, 4537 (1960).
20. Hiatt, R. R., "Frontiers of Free Radical Chemistry"; Academic Press: New York, 1980.
21. Kharasch, M. S., Nudenberg, W. and Mantell, C. J., J. Org. Chem. 16, 524 (1951).

Chemical Factors Affecting Insolubles Formation In Shale-Derived Diesel Fuel

Erna J. Beal
John V. Cooney
Robert N. Hazlett

Naval Research Laboratory
Washington, D. C. 20375-5000

Introduction

Deterioration in fuel quality with time has been a continuing problem in the utilization of middle distillate fuels. Diesel fuel instability is usually defined by the formation of insoluble sediments and gums and by the accumulation of hydroperoxides. Recent studies into the mechanisms of storage instability with middle distillate fuels have indicated that the presence of polar materials, particularly nitrogen heterocycles, can be detrimental to stability (1-4). In particular, nitrogen containing aromatics (pyrroles, pyridines, indoles, etc.) appear to be very harmful. Nitrogen heterocyclic compounds which commonly occur in middle distillate fuels include alkylated pyridines, quinolines, tetrahydroquinolines, indoles, pyrroles and carbazoles. Correlation of model dopant studies with results obtained with actual unstable fuels has indicated that the autoxidation processes are usually not isolated reactions but are sensitive to the presence of other fuel constituents. (1) Little is known about the chemical mechanisms of such interactive effects in fuel instability and possible explanations include acid/base catalysis of oxidation.

In our effort to define the stability of shale-derived diesel fuel, we have conducted gravimetric accelerated storage stability tests at 43 and 80°C using three model nitrogen compounds, 2-methylpyridine, 2,6-dimethylquinoline and dodecahydrocarbazole, as dopants in an otherwise stable shale diesel fuel. Also, information about potential interactive effects has been defined for these three model nitrogen compounds in the stable fuel in the presence of a second model dopant (a hydroperoxide, organic acid or base).

Experimental

Storage Test Techniques

The accelerated storage stability test method used has been described in detail (5). In summary, 300 ml samples of filtered fuel (doped and undoped) were stressed in the dark in 500 ml screw-cap borosilicate Erlenmeyer flasks with teflon-lined caps. All samples were run in duplicate or triplicate and appropriate blank flask/filter holder corrections were applied. Vented tests were accomplished by using modified screw caps which were drilled to hold 6 mm glass tubing (with glass wool plugs). Both filterable and adherent insolubles values were determined after

stress and these measured quantities were summed to obtain total insolubles, the values reported in the text and Tables. Hydroperoxide values were determined in stressed fuel samples following filtration through glass fiber filter paper by iodometric titrations. (ASTM D-1583-60)

Base Fuel

The base fuel was a diesel fuel marine (DFM) refined from Paraho crude shale oil by SOHIO. This fuel was produced in the Navy's Shale-II demonstration and is well characterized (5-8). It was available with (sample "D-11") and without (sample "D-1") antioxidant added. The antioxidant, 2,4-dimethyl-6-*t*-butylphenol (AO-30), was originally present at the 24 mg/liter level in fuel D-11. No other additives were present in either sample. All compounds used as dopants were pure by NMR, capillary GC, and/or melting point.

Results and Discussion

Accelerated storage stability tests were conducted at 43° and 80°C for periods of time ranging from 7 to 141 days, respectively, using three model nitrogen compounds as dopants in a stable shale diesel fuel. The three model compounds, 2-methylpyridine (2-MP), 2,6-dimethylquinoline (2,6-DMQ) and dodecahydrocarbazole (DDC) were added to samples D-1 or D-11 at concentrations of 0, 45, 135, 270 and 450 ppm N(w/v), and vented trials were also conducted at 45 and 450 ppm.

Results obtained from the gravimetric test matrix indicated that 2-MP and 2,6-dimethylquinoline were inactive in sediment promotion at all temperatures, times and concentrations employed. In all instances, the total insolubles formed never exceeded 2 mg/100 ml or 1 mg/100 ml when 2-MP or the quinoline, respectively, were added.

Large amounts of insoluble sediments were formed when DDC was added as a dopant to the shale DFM as shown in Table I. For the 43°C tests, venting of the test flasks considerably reduced the yield of solids at both 45 and 450 ppm N(w/v) of added DDC. The reaction order was less than 1.0 for both temperatures used. Longer stress times did not increase total insolubles under some stress conditions.

Autoxidation of 2-MP, 2,6-DMQ and DDC in the Presence of *t*-Butylhydroperoxide (TBHP)

The initial interaction study involved the addition of a model nitrogen compound to fuel D-11 together with a hydroperoxide as co-dopant. The hydroperoxide selected was *t*-butylhydroperoxide since it is available commercially in high purity. The goal of the experiments was to survey the importance of the accumulation of hydroperoxides in a complex fuel in influencing the formation of insolubles during stress when a particular class of nitrogen heterocycles is present.

Accelerated storage stability tests employing 2-MP, 2,6-DMQ and DDC along with TBHP as co-dopants in fuel D-11 were run at 80°C for 14 days. The gravimetric results for tests run with 2-MP and TBHP, summarized in Table 2, indicated that a slight positive interaction existed under all conditions examined. The total amount of insolubles never exceeded 2.5 mg/100 ml even when the H1 TBHP concentration was used. The concentration matrix which was studied used 2-MP at two levels: Lo 2-MP = 135 ppm N (w/v), equivalent to $9.64 \times 10^{-3}M$; and H1 2-MP = 450 ppm N ($3.21 \times 10^{-2}M$). The levels of TBHP used corresponded to the same molar concentration values.

Test results for the 2, 6 DMQ/TBHP and DDC/TBHP interactions are given in Tables III and IV, respectively. All of the dopants were added at a concentration equivalent to $3.21 \times 10^{-2}M$. Examination of these results indicates that TBHP had no effect when added as a co-dopant with 2,6-DMQ. The highest amounts of total insolubles were formed in the unvented tests where DDC and TBHP were added with almost a two-fold increase over the vented trials with the same dopants and over the tests where only DDC was present.

Autoxidation of 2-MP, 2,6-DMQ and DDC in the Presence of Organic Acids and Bases

In an extension of our study of interactive effects, two organic acids and two organic bases were examined as co-dopants in fuel D-11. This work was intended to determine whether the autoxidation of the nitrogen compounds is subject to acid or base catalysis. The four co-dopants selected for study were hexanoic acid (HA), dodecylbenzene sulfonic acid (DBSA), tri-n-butylamine (TBA), and 4-dimethylaminopyridine (4-DMAP). All of the dopants were added at a concentration equivalent to $3.21 \times 10^{-2} M$. Accelerated storage stability was assessed at 80°C for 14 days.

With 2-MP, HA and the two bases, TBA and 4-DMAP, showed no effect in the promotion of insolubles. However, the sulfonic acid, DBSA, exhibited a very strong positive interaction in both the vented and unvented tests producing over 700 mg/100 ml of insolubles (Table V). It is reasoned that 2-MP and DBSA form a salt, a polar material which is insoluble in the low polarity fuel.

Results from the interaction studies with 2,6-DMQ are shown in Table III. The two organic bases showed no synergism and HA showed a slight positive interaction producing about 2.0 mg/100 ml of insolubles. The addition of the sulfonic acid, DBSA, caused copious amounts of an opalescent tan solid to form in all the interactive flasks. This solid is very likely the sulfonate salt. There was more than 1000 mg/100 ml but the exact amount was hard to determine because of the difficulty encountered in filtering this solid.

The combination of a carboxylic acid, HA, or a sulfonic acid, DBSA, with DDC results in a strong negative interactive effect with the highest amount of sediment (14.0 mg/100 ml) produced in the vented flask of the HA/DDC interaction. The addition of TBA as a co-dopant with DDC appeared to be synergistic while the addition of 4-DMAP had a negative interactive effect (Table IV).

CONCLUSIONS

The model compound dopant studies show that the pyridine and the quinoline were inactive as sediment producers by themselves and with all co-dopants except a soluble sulfonic acid which interacted to form large amounts of insolubles. DDC formed large amounts of insolubles by itself and exhibited both positive and negative interactions with co-dopants.

ACKNOWLEDGEMENT

The authors thank the Department of Energy for sponsoring this work under contract number DE-IA-81BC10525. References to brand names were made for identification only and do not imply endorsement by DOE or NRL.

References

1. J. V. Cooney, E. J. Beal and R. N. Hazlett, Preprints, Div. of Petrol. Chem., A.C.S., 29:247-255 (1984).
2. J. W. Frankenfeld, W. F. Taylor and D. W. Brinkman, Ind. Eng. Chem. Prod. Res. Div., 22:608-614 (1983). *ibid* 615-621 and 622-627 (1983).
3. J. W. Goetzinger, C. J. Thompson, D. W. Brinkman, U. S. Department of Energy Report No. DOE/BETC/IC-83-3 (1983).
4. J. V. Cooney, E. J. Beal, M. A. Wechter, G. W. Mushrush and R. N. Hazlett, Preprints, Div. of Petrol. Chem., A.C.S., 29:1004-1014 (1984).
5. J. V. Cooney, R. N. Hazlett and E. J. Beal, U. S. Department of Energy Report No. DOE/BC/10525-4 (1983).
6. N. J. Waslik and E. T. Robinson, A.C.S. Symposium Series, 163:223-235 (1981).
7. W. A. Affens, J. M. Hall, E. Beal, R. N. Hazlett, J. T. Leonard, C. Nowack and G. Speck, A.C.S. Symposium Series, 163:253 (1981).
8. E. W. White, David Taylor Naval Ship Research and Development Center Report No. DTNSRDC-81/040 (1981).

Table I
 Total Insolubles for DFM with Added Dodecahydrocarbazole
 mg/100 ml**

ppm N (w/v)	Fuel	D-11 80°C 7 days	D-1 80°C 14 days	D-11 43°C 70 days	D-11 43°C 140 days
0		0.2	1.0	-0.4	0.1
45		46.6	38.5	26.1	49.6
45*		42.4	51.7	1.1	6.1
135		75.3	102.7	61.2	88.9
270		158.7	177.2	193.0	128.5
450		322.9	267.8	328.4	244.9
450*		220.8	271.0	99.9	140.8

* Vented

** Averages for duplicates

Table II

Total Insolubles for Stressed DFM with Added 2-MP
and TBHP
(mg/100 ml)
80° - 14 days - D-11 - duplicate tests

<u>Sample #</u>	<u>Total Insoluble</u>
Fuel Blanks	-0.2 0.0
Lo TBHP Blanks	0.0 0.1
Lo TBHP/Lo- 2-MP	0.6 1.0
Lo TBHP/Lo- 2-MP	1.5 0.9
Lo TBHP/H1- 2-MP	0.4 0.3
Lo TBHP/H1- 2-MP	0.6 0.4
H1 TBHP Blanks	0.4 0.2
H1 TBHP/Lo 2-MP	0.5 0.7
H1 TBHP/ Lo 2-MP*	1.8 2.4
H1 TBHP/H1 2-MP	1.3 0.3
H1 TBHP/H1 2-MP*	1.7 1.4

* Flasks Vented

* See Text for Concentrations

Table III

Total Insolubles for stressed DFM with
2,6-DMQ + Various Co-dopants
80°C - 14 days - D-11

Sample #	Total Insolubles, mg/100 mls				
	TBHP	4-DMAP	TBA	HA	DBSA
Blank Fuel	0.2	0.4	-0.1	0.0	0.2
2, 6-DMQ Blanks	0.4	1.5	0.6	0.5	0.3
A-2 Blanks	1.3	0.6	0.4	0.4	1.1
A-2 + 2, 6-DMQ** (unvented)	1.3	0.6	0.2	1.9	>1000.0*
A-2 + 2, 6-DMQ** (vented)	1.5	0.6	0.4	2.1	>1000.0*

* A-2: Co-dopant
Concentration: 3.21×10^{-2} M

* Gravity filtered - Dried - Taken off filter and weighed.

** Average of Triplicates; all others average of duplicates.

Table IV

Total Insolubles for Stressed DFM with DDC +
Various Co-dopants
80°C - 14 days - D-11

Sample #	Total Insolubles, mg/100 mls				
	TBHP	4-DMAP	TBA	HA	DBSA
Blank Fuel	0.0	0.3	0.1	0.0	0.2
DDC Blanks	168.5	262.3	191.8	135.2	258.2
A-2 Blanks	2.8	31.1	4.3	0.0	1.7
A-2 + DDC* (unvented)	310.4	160.8	285.5	2.1	2.3
A-2 + DDC* (vented)	176.4	165.4	291.0	14.0	3.8

* A-2: Co-dopant
Concentration: 3.21×10^{-2} M

* Average of Triplicates; all others average of duplicates.

Table V

Total Insolubles for Stressed DFM with 2-MP
 + Various Co-dopants
 80°C - 14 Days - D-11

Sample #	Total Insolubles, mg/100 mls			
	4-DMAP	TBA	HA	DBSA
Blank Fuel	0.0	0.1	0.0	2.7
2-MP Blanks	0.5	0.3	0.2	1.0
A-2 Blanks	-0.2	-0.2	0.2	0.1
A-2 + 2-MP* (unvented)	0.1	0.0	0.0	757.2
A-2 + 2-MP* (vented)	0.2	0.1	0.0	719.9

* A-2: Co-dopant

Concentration: 3.21×10^{-2} M

* Average of Triplicates; all others average of duplicates.

THE SIGNIFICANCE OF THE OXIDATION OF 2,5-DIMETHYLPYRROLE IN OXIDATIVE FUEL STABILITY

Bruce David Beaver
Department of Chemistry
Duquesne University
Pittsburgh, PA 15282

Robert N. Hazlett
Combustion and Fuels Research
Code 6181
Naval Research Laboratory
Washington, DC 20375-5000

John V. Cooney
University of Miami
School of Medicine
Miami, FL

Jay M. Watkins
GEO-Center, Inc.
Newton Falls, MA 02164

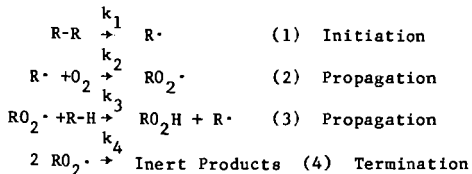
INTRODUCTION

Alkylpyrroles have been known to promote sediment formation and discoloration of petroleum distillates for over thirty years.¹⁻⁴ There has been much effort directed towards understanding the detailed mechanism of alkylpyrrole promoted sediment formation in petroleum distillates.⁽⁵⁻⁹⁾ In addition, the Fuels Section of the Naval Research Laboratory has been involved in investigating the mechanism of alkylpyrrole sediment formation in shale derived synfuels.⁽¹⁰⁻¹⁴⁾ It is the intent of this article to critically review some of the postulated mechanisms for alkylpyrrole promoted sediment formation in fuels and then to comment on the significance of these mechanisms to our overall understanding of the field of oxidative fuel stability in general.

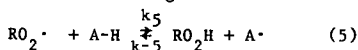
I. The Reaction of Oxygen with Organic Molecules

The fundamental chemical reactions involved in sediment formation in fuels are generally believed to start by the reaction of ground state triplet oxygen with various reactive organic molecules which are components of the fuel. There are at least two fundamentally different types of reactions that can occur between triplet oxygen and organic molecules.

By far the most common type of reaction between organic molecules and triplet oxygen is free radical initiated oxidation of organic compounds by molecular oxygen. The accepted chain mechanism which satisfactorily rationalizes this type of reaction is summarized as the following:



Where R-R is the initiator and R· and RO₂· represent the carbon radical and the chain-carrying peroxy radical respectively.(15,16) Many of the current fuel antioxidants have been developed to address this type of Scheme. For instance, the effectiveness of both phenolic and amine antioxidants can be simplistically attributed to their breaking of the radical chain as shown in (5):



A → non chain products

Where A-H represents the antioxidant.(17) If k₅ is larger than k₃ then the oxidation is inhibited until the antioxidant is consumed.

A second class of antioxidants are the so called "preventive antioxidants".(18) These include metal deactivators, UV light deactivators, and peroxide decomposers. The first two deactivators are designed to inhibit the initiation step and also inhibit the decomposition of peroxides. Peroxide decomposers, as the name suggests, destroy peroxides without generating free radicals in the process.

The second type of fundamental reaction that can occur between triplet oxygen and organic molecules has only recently been thoroughly investigated.

Thomas Bruice and coworkers have reported detailed studies on the mechanism of biological oxidation with flavoenzyme mixed function oxidases.(19) Bruice has shown that the initial mechanism for the formation of the biologically active form of the flavoenzyme mixed function oxidase [4] involves the oxidation of compounds [1] by triplet oxygen to yield the radical ion pair [2] (Scheme I). Forward reaction occurs with the collapse of [2] to form the more stable covalent intermediate [3] which can capture a proton to yield [4]. The Bruice group has very eloquently shown i) that formation of [2] is the rate determining step and ii) that the transition state of the rate limiting step is very similar in structure to [2].

In the Bruice mechanism it is important to note that structural features in the organic molecule (i.e. oxidation potential) must be such that, when coupled to the reduction of triplet oxygen, the reaction is not overly endergonic.

Sinhababu and Borchardt have recently reported polarographic and spectroscopic data which suggests the oxidation of 5,7-dihydroxytryptamine [5] involves an electron transfer from compound [5] to oxygen, resulting in radical ion pair [6] (Scheme II).(20) Recombination of superoxide with the incipient free radical would produce hydroperoxide anion [7] which upon protonation yields hydroperoxide [8]. Hydroperoxide [8] is unstable and undergoes further reaction yielding the reactive quinones [9] and [10].

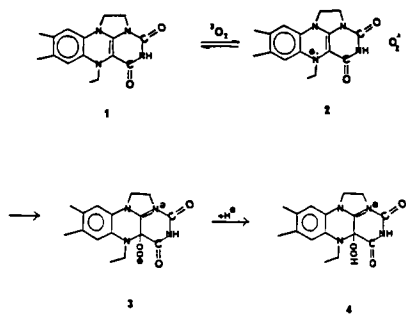
Aside from the above mentioned studies there have been few detailed mechanistic studies of the reaction of organic molecules with low oxidation potentials with ground state triplet oxygen.

II. Characteristics of DMP Sediment

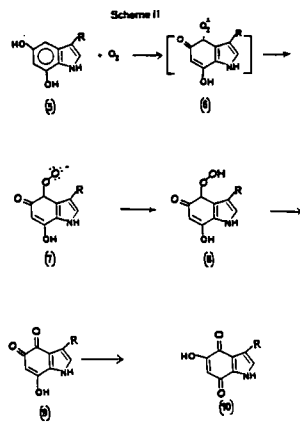
Cooney and Wechter have reported the depletion of added 2,5-DMP in a shale-derived diesel fuel correlated with oxygen uptake by the doped fuels (11). Sediment analysis data indicate that the sediment is derived from oxidation of the DMP with no incorporation of fuel constituents. In addition, analysis of the sediment derived from oxidation in a pure organic solvent also indicates the sediment is derived from DMP oxidation.

No changes were observed in the g.c. traces of stressed fuel sample with increasing length of stress. Also, stress runs in dodecane indicate the absence of any soluble oxidation products from DMP. Thus, the soluble primary oxidation

Scheme I



Scheme II



products derived from DMP are highly reactive and are rapidly converted to insoluble sediment, thereby thwarting direct attempts at their characterization.

Analysis of the sediment derived from stressing DMP doped fuels suggests the sediment arises from oxidative self condensation of the DMP (formation of dimers, trimers and tetramers). Spectroscopic analysis suggests that in the sediment the pyrrole nucleus is intact and that the CO, CO₂H, N-H, CH₂, CH₃, moieties are present. Elemental analysis of the sediment yields a molecular formula of approximately C₆H₇NO₂, regardless of the stress conditions. In addition, mass spectral studies, of the DMP derived sediment have lead Frankendorf et.al(7-9) to suggest some possible partial structures for the DMP sediment.

III. The Mechanism of Pyrrole Autoxidation

Smith and Jenson(21) have reported a detailed study of the oxidation of neat 1-alkylpyrroles. The detection of peroxide intermediates and the isolation and characterization of the oxidation products from 1-methylpyrrole, lead to the proposal that 1-alkylpyrrole reacts with oxygen by a free radical peroxy addition process (Scheme III).

Free radical reactions have also been invoked to rationalize the autoxidative oligomerization of DMP.(7-9) Li et.al. have reported esr evidence of pyrrole radicals during the oxidation of DMP and NMP (N-methylpyrrole) using fuel as the diluent. This observation lead Li et.al. to propose the partial reaction sequence shown for sediment formation (Scheme IV).(6)

This mechanism has merit in that a rationalization is provided for the observation that the rate of DMP oxidation is much more rapid than the rate of NMP oxidation (based on oxygen uptake studies). The fact that radical A can be stabilized through resonance and radical B can not, could account for the increased rate of formation of A relative to B.

One major weakness with proposing free radical mechanisms for alkylpyrrole autoxidation schemes is that in both fuels and pure organic solvents, the presence of radical chain scavenger antioxidants has little effect on the rate of alkylpyrrole oxidation.(12)

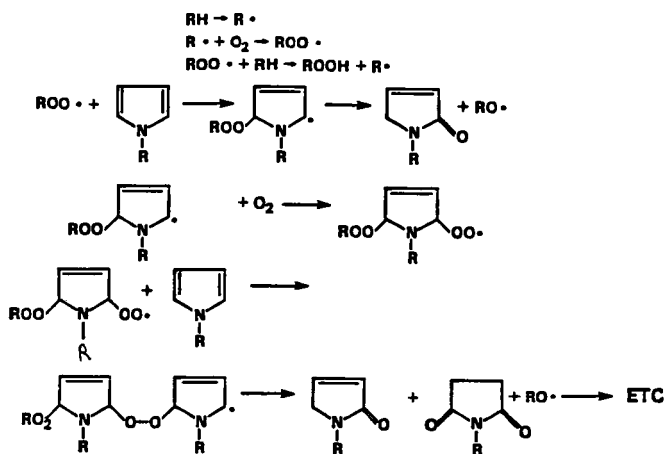
In fact, the autoxidation of DMP in 1,2,4-trichlorobenzene, in the presence of vitamin E, had only a slight depressive effect on the rate of DMP oxidation.(22) This is surprising in view of the fact the vitamin E is one of the most efficient radical scavengers known.(23)

Clearly, Li et.al.(6) have detected the presence of pyrrole radicals during the oxidation of DMP and NMP. Smith and Jenson's(21) data can be nicely rationalized in terms of the pyrrole oxidation involving radical reactions. However, our vitamin E experiment suggests that the DMP free radical intermediate observed by Li et.al. is not on the reaction coordinate leading to product formation (sediment).

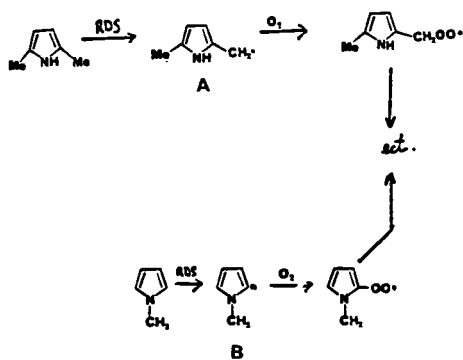
In our studies(12-14) on the mechanisms of the reaction of triplet oxygen with alkylpyrroles, several different organic solvents were utilized rather than fuels as diluent. In this manner the fundamental oxidation reaction could be studied without the potential complicating interactive effects that can occur in fuels.(10) In both fuels and pure organic solvents the oxidation of alkylpyrroles results in the formation of an intractable red-brown product. Presumably, this sediment is composed of oligomeric oxidized pyrrole nuclei (Vida Supra). In addition we have thus far found no evidence for any intermediates in the alkylpyrrole oxidation in the hydrocarbon solvents utilized in our study.

Thus our understanding of the mechanism of alkylpyrrole oxidation is based on an interpretation of our crude kinetic studies of these reactions. We have suggested, (12-14) as shown in Scheme 5, the first step of the oxidation involves

Scheme III



Scheme IV



the reversible formation of a molecular association complex between the alkylpyrrole and dissolved oxygen. This hypothesis is supported by previously published UV spectroscopic data; in addition, such association complexes between triplet oxygen and electron-rich molecules are well known(24).

The rate determining step depicted in Scheme 5 utilizes the alkylpyrrole as an electron donor and oxygen as an electron acceptor. Such a mechanistic sequence qualitatively explains why electron rich pyrroles autoxidize so much faster than pyrrole itself or than pyrroles substituted with electron withdrawing groups (25-27). Additionally, this scheme accounts for the observation that there exists a correlation between the pyrrole anodic oxidation potential and the pseudo-first-order rate constant for the oxidation(13). As already mentioned, similar redox processes have been implicated in the oxidation of dihydroflavins and tyrtamine derivatives with triplet oxygen.(19,20) The observed ESR signal reported by Li et.al. (6) during DMP oxidation can also be rationalized as arising from a strong, single-electron donor-acceptor affinity between the pyrrole and triplet oxygen (28).

As shown in Scheme 5, the charge transfer complex is postulated to be in equilibrium with an endoperoxide intermediate. Such endoperoxides are believed to be intermediates in the photochemical dye-sensitized oxidation of pyrroles(25). Such a common intermediate for both sensitized photooxidation and oxidation could thus account for the observation that many photochemical oxidations and oxidations produce the same type of oxidation products(26,27).

We have recently suggested that when the kinetic and thermodynamic parameters, for the alkylpyrrole oxidation in various hydrocarbon solvents, are compared the observed trends can be rationalized as being consistent with the mechanism proposed in Scheme 5.(14)

There is one unifying theme in the previously discussed work of Bruce(19), Borchardt(20) and our pyrrole oxidation studies.(12-14) In all of these investigations the initial step in the oxidation sequence has been suggested to involve the transfer of an electron from an organic substrate to ground state triplet oxygen. We shall classify this type of oxidation reaction as "electron transfer initiated oxidation."

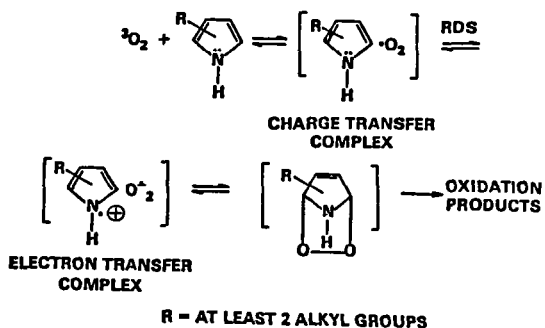
Electron transfer initiated oxidation in fuels is very complex mechanistically due to the plethora of potential interactive effects that can occur with fuel components. For instance, Frankenfeld et.al.(7-9) have shown that when certain fuels are doped with DMP and certain codopants (pyrrole or trimethylamine or certain sulfur compounds) less sediment is produced than expected during simulated storage stability tests. We have found that the oxidation of DMP in the presence of $FeCl_3$ results in a (5-10) fold increase in the rate of sediment formation.(22) Undoubtedly, much more research is necessary before we are in the position to fully understand electron transfer initiated oxidation reactions and their impact on the oxidative storage stability of fuels.

IV. Recent Developments in the Understanding of Autoxidation Reactions in Fuels

Based on stress/sediment formation studies, Frankenfeld et.al.(8), have correlated the sediment formation propensity of various aromatic nitrogen heterocycles with their structure (Scheme 6). Our oxidation studies in model fuel systems have allowed us to further probe the heterocycle structure-sediment formation relationship.

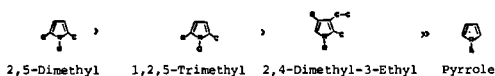
First, each heterocycle has at least two distinct oxidation pathways available. Both, free radical initiated and electron transfer initiated oxidation occurs to some extent for each heterocycle. However, the rate of each reaction pathway may be very different. The rate constant for oxidation is dependent both on the structure of the heterocycle and on the experimental conditions of the oxidation reaction. For example, we have suggested the oxidation of DMP, TMP, and kryptopyrrole (and presumably all poly alkylpyrroles) procede via an electron

Scheme V

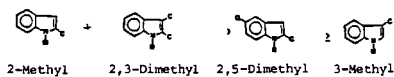


Scheme VI

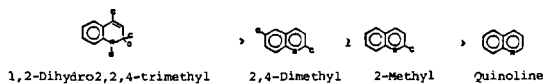
A. Pyrroles



B. Indoles



C. Quinolines



Influence of structure on reactivity of various nitrogen heterocycles toward sediment formation. Reactivity decreases from top of list to the bottom (A>B>C) and left to right. (From reference 7)

transfer initiated oxidation process. Li and Li(6) have shown that during the oxidation of DMP there is ESR evidence for the existence of DMP free radicals, presumably arising from free radical initiated oxidation. Under the experimental conditions employed in our pyrrole studies, the rate of the electron transfer initiated oxidation pathway is many times more rapid than the rate of free radical initiated oxidation. However, nitrogen heterocycles that do not have the appropriate oxidation potential to undergo electron transfer oxidation might have, in the presence of an initiator, a sufficient rate constant for free radical oxidation. Therefore, free radical initiated oxidation can also result in sediment formation if the final oxidation products are insoluble in the diluent. We have found this to be the case in the oxidation in 3-methylindole in D-11.

Second, the amount of sediment produced during oxidation is not necessarily related to the rate of oxidation. The intrinsic solubility of the products formed during the oxidation is another major factor in the amount of sediment produced during oxidation.

For instance, we have confirmed that DMP oxidation produces more sediment than the analogous oxidation of TMP with both fuel and dodecane as diluent. However, we have previously shown that the rate of TMP oxidation is more rapid than the analogous oxidation of DMP in organic solvents. Therefore, the final oxidation products of TMP must be more soluble than the corresponding DMP oxidation products.

V. The Significance of DMP Oxidation to our overall understanding of Oxidative Storage Stability of Fuels.

We believe that due to the diligent work of many research groups over the course of many years we are just starting to gain new insight into the complex chemistry involved in prolonged fuel storage. The oxidation of DMP is a very important reaction in that it is the first example of what we believe to be a significant reaction in the prolonged storage of fuel, namely, electron transfer initiated oxidation. Just how significant this mode of oxidation is in fuel chemistry is not yet fully comprehended. In principal, any electron rich organic molecule can undergo electron transfer initiated oxidation and thus promote sediment formation. Also preliminary data indicates that certain metals can catalyze electron transfer initiated oxidation.

Indeed, we are only beginning to understand the significance of this reaction in the field of oxidation storage stability of fuels. We are continuing our efforts to provide a greater degree of understanding of electron transfer initiated oxidation.

REFERENCES

1. Y.G. Hendrickson, Preprints General Papers 4(1), 55, Division of Petroleum Chemistry, 135th Meeting, ACS, Boston, MA, April 1959.
2. A.A. Oswald and F. Noel, J. Chem. and Eng. Data, 6, 294 (1961).
3. R.B. Thompson, J.A. Chenicek, L.W. Druge, T. Symon, Ind. Eng. Chem., 43, 935 (1951).
4. J.W. Goetzinger, C.J. Thompson, D.W. Brinkman, "A Review of Storage Stability Characteristics of Hydrocarbon Fuels, 1952-1982," Dept. of Energy Report No. DOE/BETC/1C-83/3, October 1983.
5. M.C. Loeffler, N.C. Li, Fuel, 64, 1047 (1985).
6. J. Li, N.C. Li, Fuel, 64, 1041 (1985).
7. J.W. Frankenfeld, W.F. Tavior, D.W. Brinkman, Ind. Eng. Chem. Prod. Res. Dev., 22, 608 (1983).

8. *ibid* p. 615.
9. *ibid* p. 622.
10. J.V. Cooney, E.J. Beal, B.D. Beaver, *Fuel Science & Technology Int'l.*, 4, 1 (1986) and references cited.
11. J.V. Cooney, M.A. Wechter, *Fuel*, 65, 433 (1986).
12. J.V. Cooney, R.N. Hazlett, *Heterocycles*, 22, 1513 (1984).
13. B.D. Beaver, J.V. Cooney, J.M. Watkins Jr., *Heterocycles*, 23, 2847 (1985).
14. B.D. Beaver, J.V. Cooney, J.M. Watkins Jr., *Heterocyclic Chem.*, in press (1986).
15. F.R. Mayo, *Acc. Chem. Res.*, 2, 193 (1968).
16. K.U. Ingold, *Chem. Rev.*, 61, 563 (1961).
17. L.R. Mahoney, *Angew. Chem. Internat. Edit.*, 8, 547 (1969).
18. J.A. Howard, "Homogeneous Liquid Phase Autoxidation," in "Free Radicals," J.K. Kochi, ED., 1973, Vol. 2.
19. G. Eberlein and T. Bruice, *J. Am. Chem. Soc.*, 105, 6685 (1983).
20. A.K. Sinhababu and R.T. Borchardt, *J. Am. Chem. Soc.*, 107, 7618 (1985).
21. E.B. Smith, H.B. Jenson, *J. Org. Chem.*, 32, 3330 (1967).
22. B.D. Beaver, unpublished data.
23. G.W. Burton, K.U. Ingold, *J. Am. Chem. Soc.*, 103, 6472 (1981).
24. D.F. Evans, *J. Chem. Soc.*, 345 (1953).
25. In aprotic solvents alkylpyrroles generally have oxidation potentials (-0.8 V vs. SCE) that are very close in energy to the reduction potential of triplet oxygen (-.8V vs. SCE) [22,23]. However, N-alkyl or pyrroles that contain withdrawing groups have oxidation potentials much more negative than -.80V vs. SCE [22,24]. Therefore, the oxidation of these pyrroles would not be expected to occur by way of the electron-transfer initiated oxidation depicted in Scheme 4.
26. A.F. Diaz, A. Martinez and K.K. Kanazawa, *J. Electroanal. Chem.*, 130, 181 (1981).
27. A.U. Khan, *Photochemistry and Photobiology*, 28, 615 (1978).
28. P.D. Bartlett, A.A.M. Roof, R. Subramanyum, and W.J. Winter, *J. Org. Chem.*, 49, 1875 (1984).
29. C.S. Foote in "Singlet Oxygen", edited by H.H. Wasserman and R.W. Murray, Academic Press, New York, 1979.
30. D.A. Lightner, G.S. Bisacchi, and R.D. Norris, *J. Am. Chem. Soc.*, 98, 802 (1976).
31. G.L. Landen, Y.T. Park, and D.A. Lightner, *Tet.*, 39, 1893 (1983).